Soft Matter

REVIEW

View Article Online
View Journal

Cite this: DOI: 10.1039/d6sm00041j

Coupling of electrospinning and photo-induced processes for advanced nanofibrous polymeric materials: current state-of-the-art and future perspectives

Thi Nhung Vu and Alessandra Vitale *

Electrospinning is a versatile and widely adopted technique for the fabrication of nanofibrous polymeric materials with high surface area, interconnected porosity, and tunable architectures. However, conventional electrospun mats often suffer from limited mechanical robustness, poor resistance to water or solvents, and restricted control over functionality, which hampers their deployment in advanced applications. In recent years, the integration of electrospinning with photo-induced processes has emerged as a powerful strategy to overcome these limitations by enabling controlled polymerization, crosslinking, and surface functionalization under mild and spatially selective conditions. This review provides a comprehensive overview of the current state of the art in coupling electrospinning with photo-induced reactions for the design of advanced nanofibrous polymeric materials. Both *in situ* photopolymerization during fiber formation and post-spinning photo-induced crosslinking or grafting are discussed, with emphasis on the underlying chemistries, including free-radical (meth)acrylate systems, thiol–ene click reactions, photocycloaddition-based processes, and cationic photopolymerization. Representative examples spanning low-molecular-weight precursors, macromers, polymers, and hybrid organic–inorganic systems are critically analyzed to highlight structure–property–function relationships and processing–reactivity interplay. Beyond summarizing recent advances, this review outlines key challenges and future perspectives, including reaction–jet coupling, scalability, sustainability, and the development of dynamic and multifunctional fibrous systems. By framing electrospinning as a reactive manufacturing platform enabled by photochemistry, this work aims to guide future research toward the rational design and translation of next-generation nanofibrous materials for biomedical, environmental, energy, and smart-material applications.

Received 14th January 2026,
Accepted 29th March 2026

DOI: 10.1039/d6sm00041j

rsc.li/soft-matter-journal

1. Introduction

Electrospinning has emerged as a powerful and versatile technique for the fabrication of polymer nanofibers and nanofibrous assemblies with exceptionally high surface area, interconnected porosity, and tunable micro- to nanoscale morphology.[1,2] Owing to these features, electrospun materials have attracted sustained interest across a broad range of fields, including biomedical engineering, filtration, energy storage, catalysis, sensing, and smart textiles.[3] The simplicity of the process, combined with its compatibility with a wide variety of polymers and composite formulations, has contributed to the widespread adoption of electrospinning as a platform for soft and functional materials.

Despite its many advantages, conventional electrospinning also presents inherent limitations that can restrict the performance and practical deployment of electrospun nanofibers. These include limited mechanical robustness, poor resistance to water or solvents for many polymer systems, broad fiber diameter distributions, and challenges associated with post-processing, long-term stability, and large-scale production. In particular, the absence of covalent network formation in many electrospun mats results in structural fragility under mechanical stress, humid environments, or physiological conditions, which is detrimental for advanced and application-driven uses.

To address these challenges, significant efforts have been devoted to the development of reactive electrospinning strategies, in which electrospinning is coupled with chemical reactions such as polymerization or crosslinking.[4] Among these approaches, the integration of electrospinning with photo-induced processes has emerged as a particularly attractive solution. Light-driven

Department of Applied Science and Technology, Politecnico di Torino, 10129 Torino, Italy. E-mail: alessandra.vitale@polito.it

reactions enable polymerization or crosslinking to occur either *in situ* during fiber formation or as a post-spinning treatment, providing spatial and temporal control over network formation under mild conditions.[5,6] Compared to thermal or chemical curing, photo-induced processes offer advantages such as low energy consumption, rapid reaction kinetics, compatibility with temperature-sensitive substrates, and the possibility of patterning or selective activation.

In recent years, the coupling of electrospinning with photo-induced polymerization and crosslinking has enabled the fabrication of nanofibrous materials with enhanced mechanical integrity, solvent and water stability, controlled degradation, and tailored surface functionality. Importantly, this strategy has expanded the range of processable materials to include low-molecular-weight monomers, oligomers, macromers, and functional additives, while also providing powerful tools for post-spinning surface modification and hierarchical structuring. As a result, photo-assisted electrospinning has become a key enabling technology for the design of advanced nanofibrous polymeric materials with precisely engineered properties.

This review focuses on the current state of the art and emerging trends in coupling electrospinning with photo-induced processes for the fabrication and functionalization of nanofibrous polymeric materials. Both *in situ* photopolymerization during electrospinning and post-spinning photo-induced crosslinking or grafting are discussed, highlighting the underlying chemistries, processing strategies, structure–property relationships, and representative applications. Particular emphasis is placed on radical, thiol–ene, cycloaddition, and cationic photochemical systems, as well as on their integration with electrospinning to overcome key limitations of conventional fibrous materials.

It is important to note that this review does not cover photo-responsivity phenomena of electrospun nanofibers, such as fluorescence, photochromism, photocatalysis, photo-induced wettability and shape-memory effects, which have been comprehensively addressed in a recent dedicated review.[7] Instead, the present work is specifically devoted to photo-induced reactions as synthetic and processing tools for stabilizing, structuring, and functionalizing electrospun polymer nanofibers.

By providing a critical overview of recent advances and identifying current challenges and future perspectives, this review aims to serve as a useful reference for researchers working at the interface of electrospinning, photochemistry, and soft matter design.

1.1 Electrospinning

Electrospinning is a versatile, simple, and cost-effective technique for generating nanofibers and nanofibrous membranes from polymer solutions or melts, with fiber diameters ranging from nano to a few micrometers.[8,9] Generally, the electrospinning setup consists of four main components (Fig. 1): (i) a spinneret connected to a syringe containing the polymer fluid, (ii) a metering pump to regulate flow rate, (iii) a high-voltage power supply, and (iv) a grounded collector, which may be a static plate or a rotating drum. When the working voltage is applied to the spinneret, the polymer solution or melt becomes highly charged, and charges accumulate at the droplet surface at the spinneret tip. When electrostatic repulsion exceeds surface tension, the droplet deforms into a ''Taylor cone'', from which a charged liquid jet is emitted toward the grounded collector. While traveling through the air, the jet bends and stretches in a complex spiral motion due to electrostatic repulsion within the jet itself. Concurrent solvent evaporation (for solutions) or cooling (for melts) results in solidification of the jet. Finally, the solidified nanofibers are deposited randomly on the collector, forming a non-woven membrane characterized by high porosity, large surface area, and tunable micro- to nanoscale morphology.[2] Fiber characteristics can be modulated

Thi Nhung Vu

Thi Nhung Vu is a PhD candidate in the Department of Applied Science and Technology at Politecnico di Torino (Italy). She received her MSc degree in Polymers for Advanced Technologies from Université Grenoble Alpes (France) in 2023. Her current research focuses on the integration of electrospinning and photo-induced processes for the development of innovative nanofibrous membranes for water treatment applications.

Alessandra Vitale

Prof. Alessandra Vitale received her PhD in Materials Science and Technology from Politecnico di Torino, Italy, in 2014. After serving as a Research Associate at Imperial College London, UK, she joined Politecnico di Torino in 2016, where she is currently an Associate Professor. She has authored around 90 peer-reviewed publications and presented her research at numerous international conferences. Her research focuses on functional nanofibrous polymeric membranes produced by electrospinning, sustainable thermoset polymer networks and polymer-based composites, and photo-assisted strategies to tailor the properties and functionality of electrospun materials.

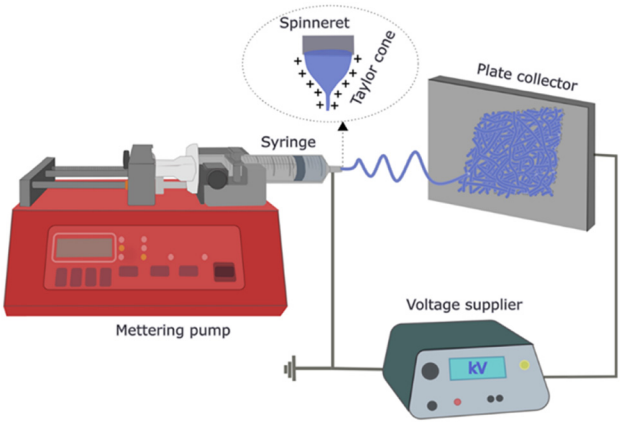

Fig. 1 General set-up of the electrospinning process.

through solution parameters (*e.g.*, viscosity, concentration, conductivity), processing conditions (*e.g.*, voltage, flow rate, tip-to-collector distance), and environmental factors such as temperature and humidity.[10]

Electrospinning is compatible with a broad range of polymers, including synthetic and natural macromolecules, blends, and polymer (nano)composites. Functional additives such as nanoparticles, small molecules, proteins, or enzymes can be directly incorporated, enabling the preparation of nanofibers with tailored optical, electrical, catalytic, or biological properties.[1] In addition to conventional single-fluid spinning, more advanced approaches such as coaxial, triaxial, and emulsion electrospinning allow fabrication of core–shell, hollow, or multicompartment fibers, offering further control over structure and function.[3]

Recent developments have expanded the processing window and scalability of the technique. Needleless electrospinning configurations employing rotating wires, drums, or discs enable higher throughput, while multi-needle arrays support parallelized production.[11] These advances have facilitated the translation of electrospun membranes into technologically relevant settings.

Owing to its structural tunability and broad material compatibility, electrospinning is now employed across diverse areas of soft matter research. Applications span filtration and environmental remediation,[12] energy storage, flexible electronics, smart textiles, catalysis, food packaging,[8] and particularly biomedical engineering,[13,14] where electrospun scaffolds, wound dressings, and drug delivery systems leverage their ability to mimic extracellular matrix-like architectures. As electrospinning continues to integrate with emerging fabrication strategies and post-processing methods, such as light-driven reactions, its relevance within soft matter science is expected to grow further.

1.2 Photo-induced reactions

In polymer science, light-driven reactions play a pivotal role in enabling and complementing traditional thermally activated processes, with applications spanning polymer synthesis, modification, and processing.[5,15] Photochemistry offers unique advantages over thermal methods, most notably wavelength-selective activation, high energy efficiency, and exquisite spatio-temporal control. A wide range of photochemical processes illustrates how polymers interact with light.[6] These include photopolymerization, in which photons directly trigger chain propagation; photo-induced polymerization, in which photoexcited species initiate free-radical or ionic polymerizations; photocrosslinking, the formation of covalent junctions between macromolecular chains; and photocuring, referring to light-induced solidification of monomeric, oligomeric, or polymeric systems.[16] Additional transformations such as photografting (light-driven graft copolymerization on polymer backbones or surfaces) and photodegradation (photo-oxidative chain scission) further highlight the breadth of photochemical pathways relevant not only to synthesis and processing but also to polymer recycling and end-of-life considerations.

The appeal of photo-induced polymerizations derives from their distinctive operational and mechanistic advantages. Light-driven reactions proceed efficiently under mild, often ambient conditions, which allows polymerization on thermally sensitive substrates, within temperature-sensitive environments, or even in the presence of biological matter. Reaction kinetics can be modulated simply by adjusting the light intensity or wavelength, and the ability to rapidly switch irradiation on and off provides unmatched temporal control compared to thermal processes. Moreover, because photon absorption is localized to specific regions, photochemical activity can be confined spatially, enabling patterning, lithography, and advanced additive manufacturing techniques such as stereolithography, digital light processing, and direct laser writing.

The chemistry underlying photo-induced reactions[17] relies on the generation of reactive species (*i.e.*, radicals, cations, or anions) *via* photoexcitation. In photo-induced free-radical polymerization, the most widely adopted mechanism, photoinitiators undergo Norrish Type I cleavage or Type II hydrogen abstraction to form radicals capable of initiating polymerization of (meth)acrylates and related vinyl monomers (Fig. 2a). (Meth)acrylate-based systems are attractive due to their broad monomer availability, fast propagation rates, and high functional-group tolerance. However, their chain-growth mechanism is often associated with oxygen inhibition, polymerization-induced shrinkage, heterogeneous network formation, and residual internal stresses, particularly under diffusion-limited conditions. Oxygen scavenging typically requires higher photoinitiator concentrations or increased light doses,[18] which may raise concerns in biomedical or biofabrication contexts.

In contrast, thiol–ene photopolymerization proceeds through a radical-mediated step-growth mechanism involving alternating propagation and chain-transfer reactions between thiol and ene functionalities (Fig. 2b). This mechanism generally yields more homogeneous network structures, reduced volumetric shrinkage, and lower residual stress compared to (meth)acrylate systems. Importantly, thiol–ene reactions exhibit significantly reduced sensitivity to oxygen, as peroxy radicals can abstract hydrogen

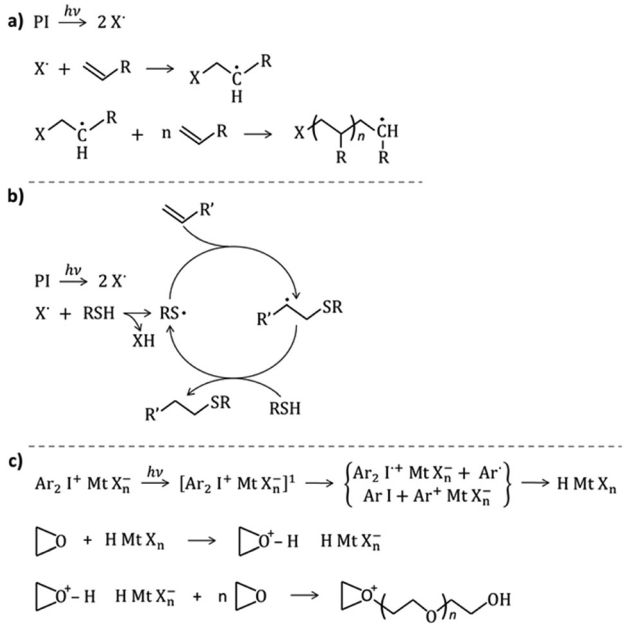

Fig. 2 Representative mechanisms of photo-induced polymerization: (a) free-radical initiation and propagation, (b) thiol–ene step-growth radical process, and (c) cationic ring-opening polymerization.

atoms from thiols to regenerate reactive thiyl species, enabling efficient curing under ambient conditions. Reaction kinetics can be tuned through ene structure: electron-rich or strained vinyl groups typically afford faster kinetics, whereas electron-poor enes or those forming stabilized radical intermediates react more slowly. Although (meth)acrylates often display very high initial propagation rates, thiol–ene systems frequently achieve rapid overall conversion (often within seconds) with improved network uniformity, which has contributed to their adoption in precision fabrication techniques.[19]

From a comparative perspective, (meth)acrylate systems offer synthetic versatility and high reactivity but may suffer from shrinkage and oxygen inhibition, whereas thiol–ene chemistries provide improved curing robustness, network homogeneity, and reduced stress at the expense of requiring stoichiometric balance and, in some cases, more complex precursor design. These complementary features underpin their widespread use in both *in situ* and post-spinning photo-reactive electrospinning strategies discussed below.

Beyond radical systems, cationic photopolymerization provides access to high-performance materials, particularly through the ring-opening polymerization of epoxides and related monomers. Upon photolysis, onium salts generate strong Brønsted acids that initiate cationic propagation, which may continue even after irradiation ceases (dark curing), greatly enhancing cure depth and efficiency in highly filled or optically dense systems (Fig. 2c). While anionic photopolymerization remains less developed due to the scarcity of suitable photobase generators and greater sensitivity to impurities, advances in photolatent base chemistry are opening new opportunities for oxygen- and moisture-tolerant processes.

In the last decade, the integration of photochemistry with advanced polymerization methodologies has transformed the synthetic landscape.[20,21] Light-driven strategies have been successfully integrated with controlled/living polymerizations and extended to other reaction pathways, enabling unprecedented control over polymer growth and architecture. These approaches leverage the precision, orthogonality, and tunability afforded by light to access complex macromolecular architectures, block copolymers, gradient structures, sophisticated constructs, and even single-chain nanostructures formed through intramolecular photodimerization.

1.3 Coupling of electrospinning and photo-induced reactions

Despite their well-established suitability for electrospinning, single-component polymeric systems often fail to meet the full set of requirements demanded by advanced applications. Synthetic polymers typically provide adequate mechanical strength but lack intrinsic bioactivity, whereas natural polymers often exhibit limited structural stability and rapid degradation, particularly in biomedical environments. To address these limitations, a wide range of polymer modifications, blends, and advanced electrospinning strategies have been developed to enhance the performance of electrospun membranes. In this context, coupling electrospinning with photo-induced reactions offers a particularly effective route to expand the structural and functional diversity of nanofibrous polymeric materials. Electrospinning is generally conducted at ambient temperature (except for melt electrospinning) and pressure, making it compatible with temperature-sensitive materials. Although the process employs high electric fields and often volatile solvents, it remains comparatively mild from a thermal and processing standpoint. Electrospinning yields fibers with high surface area and rapid solvent evaporation, features that are particularly compatible with light-driven chemistries. Photo-induced reactions can be activated during jet formation, upon fiber deposition, or as post-spinning treatments, thereby enabling multiscale control over crosslinking, network formation, and surface functionality.

A widely explored approach involves the incorporation of photoinitiators or photoactive monomers directly into the spinning solution. In such systems, UV or visible irradiation during or immediately after electrospinning induces photopolymerization or photocrosslinking, stabilizing nanofibers that would otherwise be soluble, mechanically fragile, or even flowing liquids due to low viscosity. The irradiation can occur both during or immediately after electrospinning, depending on the set-up and the processed material. Free-radical photopolymerization is the most common mechanism employed, particularly for acrylate- and methacrylate-based formulations, owing to its fast kinetics and broad monomer scope. Thiol–ene photopolymerizations have also gained attention in electrospun systems because of their reduced susceptibility to oxygen inhibition and their ability to form uniform, low-shrinkage networks. Cationic photopolymerization, especially of epoxy monomers, provides an alternative route to robust nanofibers and benefits from dark curing behavior, which can improve crosslinking efficiency in dense or thick fibrous mats.

Photo-induced reactions also enable post-spinning functionalization, including photografting, photodimerization, and photoreduction. These approaches allow precise tuning of fiber surface chemistry, the immobilization of functional molecules, or the generation of nanoparticles within the fibers, capabilities that are particularly valuable for applications in sensing, catalysis, and biomedicine.

In discussing photo-induced reactions in electrospun systems, it is important to recognize that nanofibrous mats cannot be treated as optically transparent media. Typical electrospun fiber diameters range from approximately 100 to 1000 nm, which is comparable to the wavelength of visible and near-UV light. Under these conditions, light–matter interaction is governed predominantly by Mie scattering rather than simple absorption, leading to strong diffuse scattering within the porous network.[22] The high density of fiber/air interfaces, which arise from large surface area and interconnected porosity, creates multiple refractive index discontinuities ($n \approx 1.0$ for air *vs.* $n \approx 1.4$–1.6 for polymers), leading to repeated reflection and refraction events. As a result, electrospun membranes appear opaque white and behave as highly scattering porous media.[23]

Macroscopically, light attenuation in such systems is governed by an effective attenuation coefficient that includes both absorption (μ_a) and scattering (μ_s) contributions. In most nanofibrous mats, μ_s dominates, and the optical density increases with fiber packing density and membrane thickness. Consequently, photon flux decays with depth, generating a gradient in light intensity from the irradiated surface toward the interior. Because photopolymerization rates depend on local light intensity, this spatial attenuation directly affects cure depth and crosslinking homogeneity. In thick or highly porous membranes, reduced photon flux in the inner layers may lead to lower radical generation, slower polymerization kinetics, and gradients in crosslink density across the thickness. These effects become particularly relevant in high-throughput configurations such as multi-needle or needleless electrospinning, where thick fibrous deposits are rapidly accumulated.

Importantly, the optical response of electrospun membranes is intrinsically linked to structural parameters such as fiber diameter, refractive index contrast, porosity, and thickness. Increasing fiber packing density or reducing pore size enhances the number of scattering events per unit path length, thereby increasing μ_s and reducing cure depth. Conversely, thinner mats, lower refractive index contrast (*e.g.*, through filler or solvent retention), or longer irradiation wavelengths can improve effective light penetration.

From a processing perspective, these considerations highlight that scaling up photo-assisted electrospinning is not solely a matter of increasing throughput, but also requires careful control of optical transport within the growing fibrous layer. Achieving homogeneous crosslinking in thick, highly porous, or multilayered assemblies may require optimized irradiation geometries (*e.g.*, dual-side exposure), higher-intensity or longer-wavelength sources, staged curing strategies, or chemistries capable of post-irradiation propagation.

Beyond optical transport, the non-equilibrium nature of electrospinning also raises important kinetic-mechanical considerations during ultrafast photo-crosslinking. The molecular orientation imparted to polymer chains during electrospinning is intrinsically coupled to the kinetics of photo-crosslinking, with direct consequences for the mechanical response of the resulting membranes.[24,25] Electrospinning subjects the jet to intense extensional flow, inducing chain alignment and storing elastic energy within the stretched macromolecular network. When ultrafast photo-crosslinking occurs concurrently with rapid solvent evaporation, this oriented state can be ''frozen in'', trapping the system in a mechanically strained configuration far from equilibrium.[26]

Solidification during jet flight is spatially heterogeneous. Solvent evaporation proceeds from the surface inward, leading to the formation of a partially solidified skin that undergoes continued stretching while the core remains fluid-like.[27] This radial gradient in viscoelastic properties can generate residual pre-strain at the fiber surface. Subsequent crosslinking of the inner region may continue even after fiber deposition, further locking in stress gradients.

From a kinetic perspective, when the polymerization rate exceeds the relaxation rate of the stretched polymer chains, covalent bonds form before elastic stresses can dissipate. Under these conditions, the network vitrifies in a constrained configuration,[28] leading to residual internal stresses, increased brittleness, and potential latent shrinkage upon thermal or solvent exposure. Such frozen-in stresses may compromise long-term mechanical integrity, particularly in soft or elastomeric fibrous systems where stress relaxation would otherwise contribute to toughness.

Mitigation strategies include moderating irradiation intensity or implementing ''soft-start'' protocols, in which gradual light exposure allows partial chain relaxation prior to rapid network formation and vitrification.[29,30] Controlling the relative timescales of chain relaxation, solvent evaporation, and crosslinking is therefore critical to balancing structural fixation with mechanical resilience in photo-assisted electrospinning.

Beyond internal stress considerations, photo-induced crosslinking also plays a crucial role in permanently fixing the molecular anisotropy generated during jet stretching. During electrospinning, polymer chains are subjected to intense deformation arising from (i) shear stresses near the spinneret and (ii) strong Coulombic and extensional forces generated by the applied electric field. These forces induce significant chain alignment along the jet axis, leading to pronounced molecular orientation within the developing fibers.[31] The final degree of orientation reflects the competition between extensional flow, which stretches and aligns chains, and entropic relaxation, which drives the system back toward an isotropic random-coil configuration.[32]

In conventional (non-reactive) electrospinning, molecular ordering may be partially preserved through crystallization or rapid vitrification. In highly crystalline polymers, oriented nuclei can form during jet stretching, and subsequent crystal growth constrains chain mobility, limiting relaxation.[24]

In weakly crystalline or amorphous systems, rapid solvent evaporation can kinetically trap oriented chains by inducing vitrification.[33] However, in these cases, orientation is not thermodynamically fixed and may relax over time under thermal, mechanical, or solvent exposure. In reactive electrospinning, photo-induced crosslinking introduces covalent bonds while the chains are still in a stretched, non-equilibrium state.[34] If crosslinking occurs on timescales shorter than orientation relaxation, the aligned configuration becomes permanently "locked" into the network architecture. This covalent fixation suppresses entropic recoil and prevents return to a random-coil conformation after deposition. As a result, reactive electrospinning enables permanent stabilization of molecular anisotropy, distinguishing it fundamentally from purely physical fiber formation mechanisms.

Overall, integrating photo-induced processes with electrospinning offers a versatile platform for tailoring fiber morphology and functionality, supporting the development of advanced nanofibrous materials with improved stability, hierarchical structuring, and stimuli-responsive behavior. However, reactive electrospinning must be viewed as a strongly non-equilibrium process in which light transport, solvent evaporation, chain relaxation, and crosslinking kinetics are tightly coupled. Electrospun mats behave as highly scattering, optically diffusive media, while ultrafast network formation can freeze internal stress and molecular anisotropy into the fiber architecture. Accounting for these coupled optical and kinetic-mechanical effects is therefore essential to achieve uniform network formation, controlled structure–property relationships, and reliable scalability of photo-assisted electrospinning platforms.

2. Electrospinning and *in situ* photopolymerization

The integration of electrospinning with *in situ* photopolymerization represents a powerful strategy to expand the range of processable materials and to precisely control the solidification and stabilization of nanofibrous structures. In this combined approach, light irradiation is applied during fiber formation (*i.e.*, jet flight) or immediately after deposition (Fig. 3a), enabling photo-induced reactions to occur synchronously with electrospinning. Depending on the molecular characteristics of the precursor system, irradiation can trigger either polymerization (build-up of long polymer chains from monomers/oligomers) or crosslinking (network formation within pre-existing polymers), resulting in solid fibers with tailored structure and properties.

When applied to low-molecular-weight systems, *in situ* photopolymerization enables electrospinning of precursors that are liquid at room temperature, such as monomers, oligomers, or macromonomers. In these cases, the electrospinning jet is generated from a low-viscosity formulation, often assisted by additives or carrier polymers, and irradiation triggers photo-induced polymerization during jet flight or immediately upon deposition. Rapid covalent network formation leads to fiber solidification

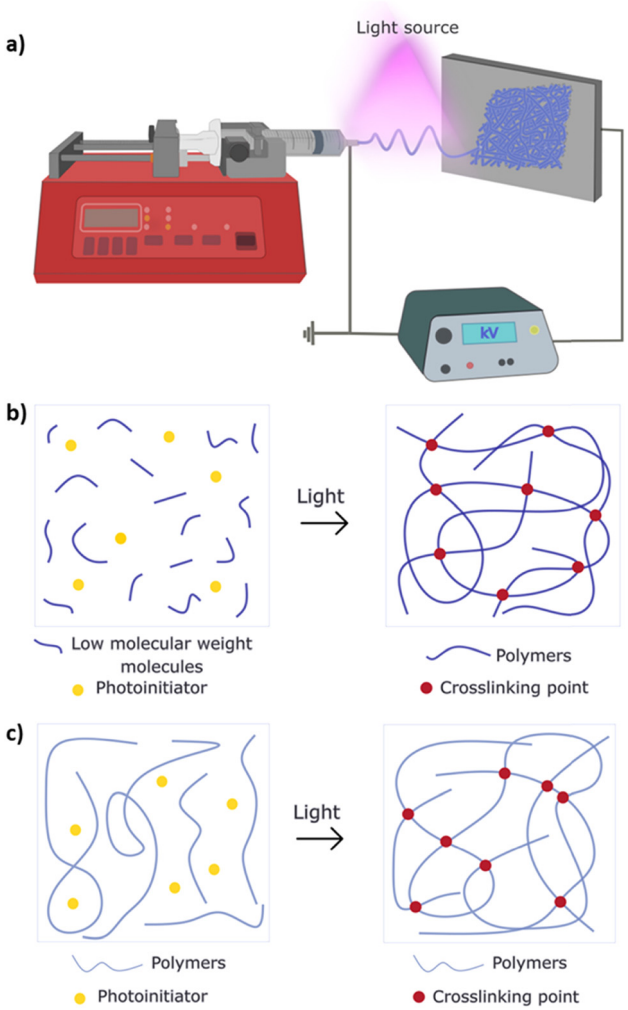

Fig. 3 Schematic of the electrospinning process coupled with *in situ* irradiation: (a) set-up, (b) photo-induced chemical modification for low molecular weight monomers, and (c) higher molecular weight systems.

during processing, effectively converting liquid precursors into stable thermoset nanofibers (Fig. 3b). This approach is particularly attractive for solvent-free or solvent-minimized processing and grants access to fibrous materials that are otherwise difficult to obtain by conventional electrospinning.

By contrast, when *in situ* irradiation is applied to polymeric systems, the fibers are typically produced by conventional solution- or melt-electrospinning, and light exposure primarily induces photocrosslinking rather than chain-growth polymerization (Fig. 3c). Network formation within and/or between fibers enhances mechanical integrity, solvent and humidity resistance, thermal stability, and long-term morphological retention. This strategy is especially valuable for water-soluble polymers, elastomers, and functional blends that require stabilization to preserve fiber structure under application-relevant conditions.

From a soft matter perspective, the extreme confinement experienced by polymer chains within the electrospinning jet and nascent fibers fundamentally alters reaction kinetics and

network formation, leading to photo-induced processes that differ markedly from their bulk counterparts. Accordingly, the following subsections address the coupling of electrospinning and *in situ* photopolymerization separately for low-molecular-weight precursors and polymeric systems, emphasizing their distinct processing requirements and resulting material properties.

2.1 Processing of low molecular weight molecules

Conventional electrospinning, whether from melts or solutions, typically relies on polymers of sufficiently high molecular weight, viscosity, and chain flexibility to enable stable jet formation. These requirements inherently limit the scope of materials suitable for electrospinning. Consequently, increasing attention has been directed toward processing low-molecular-weight molecules, either as primary precursors or as functional modifiers. However, these systems often lack the viscosity, conductivity, or surface tension required for defect-free spinning, so careful tuning of the spinning dope is essential. Coupling electrospinning with *in situ* photopolymerization provides an effective way to overcome these constraints. In particular, integrating electrospinning with rapid photo-induced polymerization/crosslinking can yield thermoset fibers directly from small molecules or oligomers, often without solvents, elevated temperatures, or post-processing, making this strategy attractive as a greener and energy-efficient route. A key practical requirement is that curing kinetics must be fast enough to match continuous fiber formation. During electrospinning, the jet experiences rapid acceleration and complex velocity variations. After leaving the Taylor cone at relatively low speeds, the jet undergoes elongation and whipping instabilities, reaching axial velocities typically on the order of 1–15 m s^{-1}, while local transverse velocities during whipping can reach several tens of m s^{-1}.[8,35] Considering typical tip-to-collector distances of 10–20 cm, the overall jet flight time is therefore on the order of 10–100 ms. For *in situ* photopolymerization of low-molecular-weight precursors, the characteristic curing time must be comparable to or shorter than this timescale to ensure sufficient network formation before fiber deposition and relaxation. If polymerization is significantly slower, the jet may undergo excessive thinning, bead formation, or loss of structural integrity.

Simultaneously, solvent evaporation and extensional thinning dramatically reduce the jet cross-section during flight. The final cross-sectional area of the dried fiber can be several orders of magnitude smaller than that of the initial jet, typically resulting in fiber diameters ranging from the nanoscale to several micrometers, depending on formulation and processing conditions.[8,36] Notably, when electrospinning low-molecular-weight systems, particularly under solvent-free or highly concentrated conditions, the achievable diameters are often in the micrometer range due to limited chain entanglement and higher effective viscosity, as illustrated in Fig. 4. This highlights the delicate balance between rheology, elongational flow, and curing kinetics in reactive electrospinning of small-molecule precursors.

Importantly, electrospinning combined with photo-induced reactions represents a strongly non-equilibrium process, in which rapid solvent evaporation, intense extensional flow, and millisecond-scale irradiation collectively dictate network formation pathways that differ fundamentally from bulk or equilibrium curing conditions.

A common route to improve electrospinnability is compositional tuning through conductive additives or rheology modifiers. For example, Zhu and co-workers electrospun two commercial multifunctional acrylate monomers (*i.e.*, hexa-functional acrylic polyester and tri-functional aliphatic urethane acrylate) by integrating electrospinning with *in situ* photopolymerization. To overcome the inherently low conductivity of the solutions, tetrabutylammonium bromide was added (1–10 wt%), resulting in increased conductivity and enabling the formation of continuous, uniform fibers.[37]

Low-molecular-weight species can also be exploited as reactive building blocks to tailor the mechanical response of electrospun networks. The group of Ellison, for example, integrated thiol–ene photopolymerization with electrospinning to produce solvent-free, crosslinked elastomeric fibers from multifunctional acrylate and thiol monomers. An optimized acrylate-to-thiol ratio provided the appropriate viscosity for stable jet formation and enabled rapid *in situ* curing, resulting in defect-free fibers. The obtained single fibers exhibited elongations at break of 8–12% and ultimate tensile strengths of approximately 80–120 MPa.[38] Replacing the acrylate monomers with vinyl

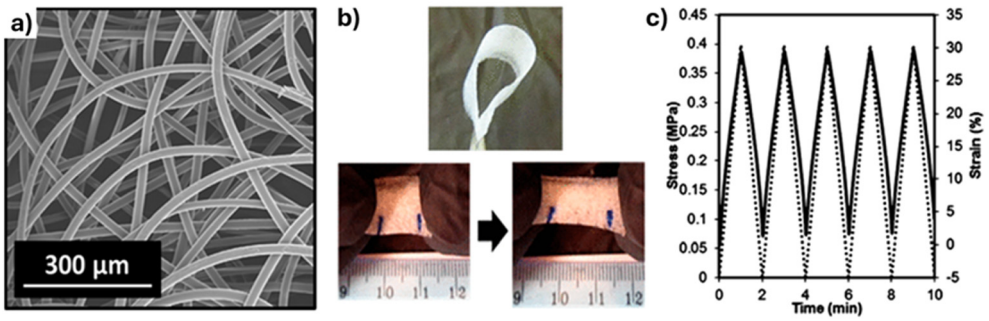

Fig. 4 Highly stretchable thiol–ene thermoset fibrous non-wovens: (a) SEM and (b) digital images of PETT/TVE non-woven mat showing its flexible and stretchable nature; (c) stress/strain cycling behavior (at 20 °C, stress: dotted line, strain %: solid line). Figure adapted from ref. 39 with permission from American Chemical Society, Copyright © 2014.

ethers led to even faster curing and more homogeneous network formation. Moreover, the inclusion of a small amount of high-molecular-weight poly(methyl methacrylate) (PMMA, 0.6 wt%) increased solution elasticity and produced fibers with excellent recovery under cyclic loading (Fig. 4).[39] Related solvent-free and heat-free elastomeric fibers were reported by the group of Vitale using liquid polybutadiene and polybutadiene-*graft*-maleic anhydride. Electrospinning was coupled with thiol–ene photopolymerization using a trifunctional thiol crosslinker, while oleic acid served as a polar additive to adjust viscosity and charge density. Irradiation initiated a rapid and chemically rich process involving thiol–ene crosslinking as well as oxidation of the polybutadiene backbone and esterification of maleic anhydride moieties. The resulting membranes exhibited excellent morphological stability, high insolubility, good thermal resistance, and a pronounced hydrophobicity.[40]

In parallel with these developments, the drive toward sustainable materials have stimulated interest in low-molecular-weight photocurable monomers derived from renewable feedstocks. Vegetable-oil derivatives such as acrylated epoxidized soybean oil (AESO) can be electrospun and photopolymerized into fibrous networks when formulated with multifunctional thiols. Incorporation of dipentaerythritol pentaacrylate, which provides a higher density of acrylate functions than AESO, improved curing kinetics, crosslinking efficiency, and overall fiber quality.[41] Carbohydrate-derived dienes (*e.g.*, isosorbide 10-undecenoate and glucarodilactone 10-undecenoate) have similarly been combined with thiols to generate fibers containing up to 94% biobased carbon, with mechanical properties readily tuned *via* monomer ratio.[42]

Low-molecular-weight photoactive components have also been used to tune wettability and biointeractions. Poly(ethylene glycol) (PEG) acrylate and methacrylate monomers, in particular, are widely employed to increase hydrophilicity and improve biological response owing to their surface properties, biocompatibility, and straightforward photo-induced network formation. Incorporating poly(ethylene glycol) methacrylate (PEGMA) into polyurethane (PU) enabled the fabrication of nanofibrous vascular scaffolds with markedly reduced water contact angles (from 118° for pure PU to 20° for a PU/PEGMA 50/50 blend), while the fibrous morphology remained largely unchanged despite the presence of the photoactive component.[43] Rapid network formation under UV irradiation was confirmed, and the enhanced hydrophilicity promoted improved cell adhesion.[44] Similarly, poly(ethylene glycol) diacrylate (PEGDA) was used to tune polyvinylidene fluoride (PVDF) membrane wettability, achieving crosslinking efficiencies above 80% and enabling a transition from hydrophobic to superhydrophilic behavior with increasing PEGDA content.[45]

The architectural versatility of low-molecular-weight precursors also enables the fabrication of core–shell fibers, most commonly through coaxial electrospinning, in which two solutions are delivered independently through a coaxial needle. For example, Miranda *et al.* encapsulated aniline in the fiber core while incorporating an oxidizing agent (ammonium persulfate) into a photocrosslinkable acrylamide/acrylic acid shell, enabling localized *in situ* polymerization of polyaniline within the nanofibers.[46] Alternatively, core–shell architectures can also be obtained using a single spinneret *via* phase separation. When incompatible polymeric components are processed, spontaneous phase separation during jet formation can give rise to core–shell morphologies, which can be "fixed" if at least one phase is photocurable (Fig. 5a). Ma and colleagues electrospun a polyvinylpyrrolidone (PVP)/thiol–ene mixture and irradiated the jet in flight, yielding a PVP-rich core and a photocured shell when the PVP : thiol–ene mass ratio reached 3 : 1.[47] A similar strategy was used to fabricate polyacrylonitrile (PAN)/polydimethylsiloxane (PDMS) core–shell fibers: poor miscibility between PAN and acrylic PDMS drove phase separation during electrospinning, while simultaneous photopolymerization stabilized the PDMS shell. Well-defined core–shell structures were achieved at a PAN/PDMS mass ratio of 2 : 1 (Fig. 5b).[48] Beyond morphology control, *in situ* photochemistry has been used to stabilize semicrystalline polymer composites. Poly(ε-caprolactone) (PCL)/polyhedral oligomeric silsesquioxane (POSS) composite fibers with enhanced structural stability were fabricated by integrating electrospinning with thiol–ene photochemistry. During electrospinning, acrylic-functionalized POSS and multifunctional thiols were excluded from the PCL crystalline phase and reacted preferentially within the

Fig. 5 Core–shell fiber architecture generated through phase separation and photopolymerization during electrospinning: (a) schematic representation of the process; (b) TEM images of PAN/PDMS nanofibers prepared at a 2 : 1 mass ratio. Figure reproduced from ref. 48 with permission from Elsevier B.V., Copyright © 2017.

amorphous regions under UV irradiation, effectively "locking" amorphous PCL chains and improving fiber stability.[49]

Finally, coupling electrospinning of low-molecular-weight precursors with photoreactions shows considerable promise for biomedical applications. For example, electrospun poly(decanediol-*co*-tricarballylate) meshes exhibited high porosity (~78%) and supported robust cell adhesion and proliferation, outperforming particulate-leached controls.[50] Nanofibrous hydrogels are also promising because the fibrous format offers abundant anchoring sites and improved mass transport compared with bulk hydrogels; however, conventional hydrogels are typically non-spinnable because their crosslinked networks swell in water without dissolving. One solution is to electrospin precursor (monomer/oligomer) mixtures prior to gelation and then photocure the fibers. Pre-oligomerized 2-hydroxyethyl methacrylate (HEMA), for example, yielded photocured pHEMA fibers (100–500 nm diameter) that swelled substantially in water while retaining elasticity.[51] Hybrid fibers combining hydrogel formation with electroactive components have also been demonstrated: electrospinning was coupled with *in situ* photopolymerization and concurrent oxidative polymerization of aniline to obtain conductive, elastic fibrous actuators with tunable mechanical behavior, highlighting opportunities for bioactuation and soft robotics.[52]

Overall, *in situ* photopolymerization enables low-viscosity monomers/oligomers to be processed into robust nanofibers by coupling jet formation with rapid network build-up, offering a direct route to solvent-free or solvent-minimized thermoset fibrous materials with tunable structure and function. The examples described clearly illustrate how nanoscale fiber morphology, network topology, and crosslinking density are intrinsically coupled, giving rise to emergent mechanical, transport, and biological properties that are unique to nanofibrous soft matter systems.

2.2 Processing of polymeric systems

Although polymers are generally well suited for electrospinning, electrospun polymer membranes may exhibit limited thermal resistance and poor environmental stability (*e.g.*, sensitivity to water, humidity, or solvents), which constrains their use under demanding conditions. Photo-induced processes provide a convenient route to crosslink or chemically modify polymer structures, thereby improving mechanical integrity, thermal performance, solvent resistance, and long-term durability.

Polyimide (PI) is a representative high-performance fiber-forming material: its aromatic heterocyclic backbone provides outstanding thermal stability, mechanical robustness, and biocompatibility. Electrospun PI fibers can be produced from pre-imidized soluble polyimides (SPI), but these materials may suffer from limited solvent resistance and environmental durability. UV-assisted electrospinning has therefore been explored as a strategy to stabilize SPI fibers through *in situ* photocrosslinking. Qui *et al.*[53,54] demonstrated that fibers prepared from a photosensitive SPI retained high thermal stability (>500 °C) irrespective of UV exposure, while

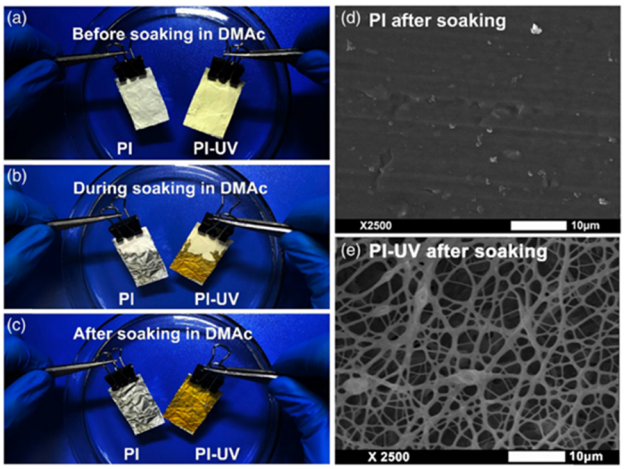

Fig. 6 Solvent-resistant polyimide fibrous membranes obtained by UV-assisted electrospinning: (a)–(c) immersion tests comparing the solvent resistance of PI fibers produced by conventional electrospinning and PI-UV fibers prepared with simultaneous photocrosslinking; (d) and (e) SEM images of the corresponding samples after immersion. Figure reproduced from ref. 54 with permission from Wiley Periodicals LLC., Copyright © 2020.

UV-treated fibers displayed markedly enhanced solvent resistance. When immersed in *N*,*N*-dimethylacetamide (DMAc), non-irradiated PI fibers dissolved rapidly, whereas UV-treated fibers retained their morphology with only minor shrinkage, confirming the formation of a robust crosslinked architecture (Fig. 6).[54] In a related study, the same group implemented UV-assisted electrospinning of PI ultrafine fibrous membranes from ester-type negative photosensitive PIs, using diethylene glycol diacrylate as crosslinker, followed by thermal imidization at 350 °C under nitrogen. UV-induced crosslinking was necessary to preserve the fibrous morphology during imidization, and enhanced the solvent resistance of the membranes.[55]

A similar stabilization concept has been applied to polyethyleneimine (PEI), a versatile cationic polymer whose electrospun membranes can suffer from solvent-induced leaching. This limitation was assessed by introducing photocrosslinkable groups *via* functionalization of linear PEI with glycidyl methacrylate. To ensure stable jet formation, a small amount (2 wt%) of high-molecular-weight PVP was added as a chain-entanglement enhancer, followed by rapid UV-induced crosslinking. By adjusting the degree of methacrylation and irradiation conditions, membrane stability, solubility, and mechanical performance could be systematically tuned.[56]

In biomedical contexts, combining electrospinning of polymeric systems with photo-induced crosslinking has enabled fibrous hydrogels, wound dressings, and drug-delivery materials with improved stability and function. In a representative example, Cho *et al.*[57] fabricated electrospun fibrous hydrogels featuring a double-network architecture. Double networks, which consist of interpenetrating physically and chemically crosslinked networks, are particularly effective in enhancing mechanical strength, toughness, and resistance to deformation. In this system, agarose formed the first network through physical

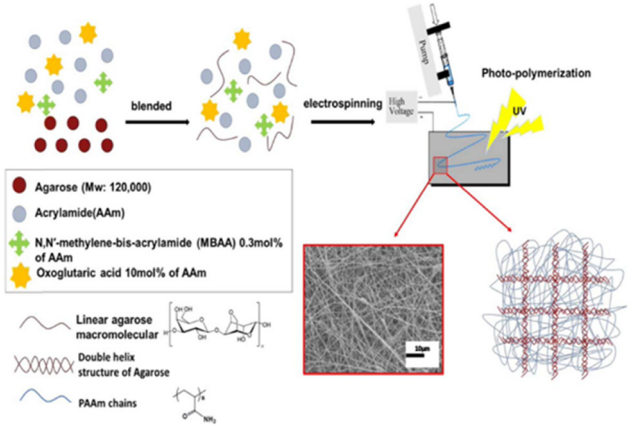

Fig. 7 Electrospinning and photocrosslinking for the fabrication of double network agarose/PAAm nanofibers. Figure reproduced from ref. 57 with permission from Wiley Periodicals Inc., Copyright © 2015.

gelation, while polyacrylamide (PAAm) constituted the second network *via* UV-induced chemical crosslinking (Fig. 7). Simultaneous electrospinning and UV exposure produced uniform fibers (down to ~187 nm diameter) and delivered mechanical and thermal performance superior to single-network agarose and uncrosslinked agarose/PAAm membranes.[57]

Photocrosslinking has also been used to tailor drug release by stabilizing hydrophilic domains in composite fibers. For instance, PU/PEGDA nanofibers with monolithic, blended, and coaxial core–shell architectures were prepared to modulate meloxicam release. UV curing stabilized PEGDA-rich regions, reducing swelling and enabling more controlled release profiles in core–shell designs.[58] Beyond this example, photo-crosslinked nanofibrous systems have been engineered to provide stimuli-responsive release: a 3D reversible gel-like nanofibrous mat based on a pH-responsive methacrylate copolymer enabled sustained, pH-controlled drug release for >80 h, with release kinetics dependent on environmental pH.[59] A related strategy has recently been applied to liver-targeted chemotherapy through the development of galactose-decorated core–shell nanofibers fabricated by coaxial electrospinning combined with *in situ* photopolymerization (Fig. 8). In this design, the fiber core consisted of N-succinyl chitosan (NSC), which provided pH responsiveness and functional groups suitable for electrostatic loading of the anticancer drug doxorubicin. The shell was formed from a photocrosslinkable copolymer of poly(vinyl alcohol) grafted with glycidyl methacrylate (PVA-*g*-GMA) and galactose-based acrylamide (Gal-acryl), simultaneously protecting the drug-loaded core and enabling liver-specific targeting *via* galactose-based interactions (Fig. 8). The resulting nanofibers exhibited enhanced drug release under tumor-mimicking acidic conditions, negligible hemolysis, and time-dependent cytotoxicity, highlighting their potential as a scalable and targeted platform for chemotherapeutic delivery.[60]

For wound-dressing materials, photo-induced crosslinking has been particularly valuable to stabilize polysaccharide-based fibrous networks in aqueous environments. The aqueous instability of maleinated hyaluronate (MHA) was mitigated by forming a photocrosslinked network with methacrylated poly(vinyl alcohol) (MPVA): at an MHA/MPVA ratio of 25 : 75, uniform bead-free fibers were obtained, showing low cytotoxicity and supporting cell adhesion and proliferation.[61] Comparable strategies with maleinated chitosan (MCS) confirmed that water-stable fibrous structures require appropriate blending ratios with MPVA.[62] Along similar lines, methacrylated dextran

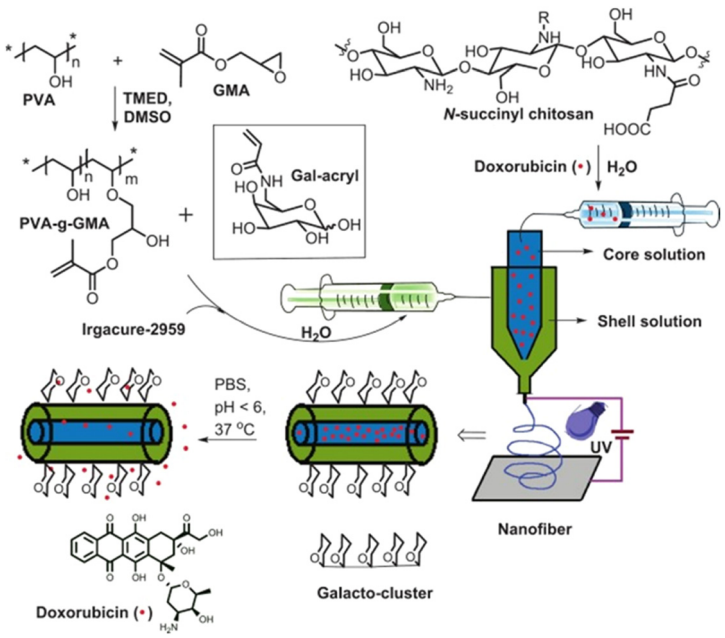

Fig. 8 Photocrosslinked stimuli responsive galactose-decorated core–shell nanofibers fabricated by coaxial electrospinning combined with *in situ* photopolymerization. Figure reproduced from ref. 60 with permission from Elsevier B.V., Copyright © 2025.

has been used to photocrosslink polylactic acid (PLA)/dextran scaffolds, allowing hydrophilicity tuning and controlled effects on cell attachment, differentiation, and biological activity.[63]

Elasticity and mechanical resilience are also central requirements for soft-tissue scaffolds and compliant vascular grafts. A recent study reported electrospun membranes with high resilience prepared by blending electrospinning of PCL with methacrylated poly(glycerol sebacate) (PGS) and *in situ* photocrosslinking using PEGDA. The resulting membranes showed minor hemolysis, low platelet adhesion, and favorable cytocompatibility; in wet conditions, compositions with PCL/PGS mass ratios of 5/5 or 4/6 exhibited reduced modulus and reversible deformation, with compliance comparable to human saphenous vein.[64] In a related approach, *in situ* photocrosslinking has been combined with wet electrospinning (*i.e.*, electrospinning into a liquid coagulation bath rather than onto a solid collector). Collecting fibers in a non-solvent bath can reduce instantaneous drying, promote controlled phase inversion and swelling, and facilitate concurrent or subsequent chemical reactions (including crosslinking). Using this strategy, Jeshvaghani *et al.* fabricated elastomeric scaffolds from blends of PCL and its photocrosslinkable derivative polycaprolactone fumarate (PCLF). By varying the PCL/PCLF ratio and the concentration of the photoinitiator, the authors identified conditions that balanced morphology, crosslinking density and elastomeric performance: bead-free fibers were obtained when PCLF exceeded 70 wt%, and swelling decreased with increasing photoinitiator content, consistent with higher crosslink densities.[65]

Composite electrospun scaffolds incorporating inorganic fillers have been extensively explored as a means to enhance both mechanical properties and functional performance, including biological activity and adsorption capability. For instance, nanofiber scaffolds prepared by blending hydroxyapatite modified with 4-vinylbenzene boronic acid into poly(vinyl alcohol) (PVA), followed by collagen surface deposition, exhibited excellent cell adhesion and proliferation, underscoring their potential for tissue engineering applications.[66] Similarly, incorporating Si–Mg co-doped fluorapatite nanoparticles (0, 5, and 10 wt%) into PCLF/gelatin fibers resulted in composite membranes with enhanced mechanical performance and controlled degradation behavior, making them suitable for guided bone and tissue regeneration. The nanoparticles were uniformly distributed along the fibers (Fig. 9), with mechanical properties optimized at 5 wt% loading, while higher contents (10 wt%) significantly accelerated membrane degradation. Cell studies confirmed good biocompatibility, with cells readily adhering to and proliferating on the composite membranes.[67] Beyond biomedical applications, nanocomposite electrospun fibers have also been developed for environmental remediation. In one example, a metal–organic framework was decorated onto UV-crosslinked PVA nanofibers, where crosslinking was initiated during electrospinning using TiO_2 and ZnO as photocatalysts in combination with citric acid as a crosslinker. While swelling and solubility depended on formulation parameters, incorporation of the metal–organic framework significantly increased the specific surface area and enhanced phosphate adsorption performance.[68]

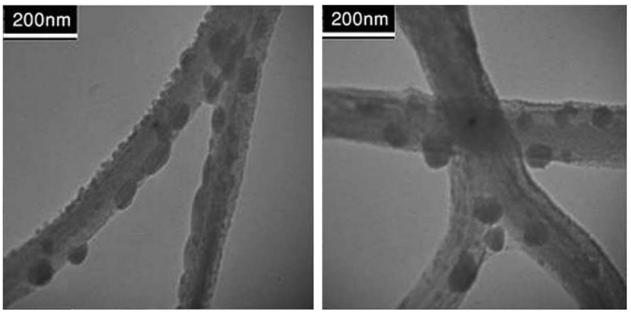

Fig. 9 Composite electrospun fibers: TEM images of the PCLF/gelatin membrane containing Si–Mg co-doped fluorapatite nanoparticles. Figure adapted from ref. 67 with permission from Elsevier B.V., Copyright © 2019.

Finally, dual-crosslinking strategies based on UV-photocrosslinking and sol–gel processes have been implemented by Mentbayeva *et al.* for electrochemical energy-storage applications. A PVA-based dual-crosslinked nanofibrous membrane was developed as matrix for gel polymer electrolytes by combining maleated PVA (PVA-MA), PEGDA, and tetraethyl orthosilicate (TEOS). UV crosslinking of PVA-MA and PEGDA was followed by sol–gel crosslinking of TEOS (Fig. 10), yielding membranes with uniform morphology, enhanced mechanical strength, improved ionic conductivity (outperforming commercial separators and pure PVDF), and superior liquid retention.[69] In a related separator design, photo-crosslinked lignin/PAN membranes were developed for safer lithium-ion batteries. Alkali lignin was maleated to enhance reactivity and mechanical properties, then blended (up to 30 wt%) into UV-curable formulations containing PEGDA and hydrolyzed 3-(trimethoxysilyl)propyl methacrylate (HMEMO) as crosslinkers, with PAN as the carrier polymer. UV-assisted electrospinning produced crosslinked membranes featuring a three-dimensional, highly porous, and interconnected fibrous network. These separators exhibited high ionic conductivity, elevated discharge capacity, excellent rate performance, and enhanced thermal and mechanical stability, highlighting the effectiveness of dual crosslinking for advanced energy-storage materials.[70]

Collectively, these examples demonstrate that irradiation during electrospinning enables controlled photocrosslinking of polymer-derived nanofibers, enhancing durability and functional performance while preserving the defining morphological features of electrospun architectures.

3. Photocrosslinking of electrospun mats

As an alternative to *in situ* photopolymerization during electrospinning, light irradiation can also be applied after fiber deposition, as schematically illustrated in Fig. 11. In this case, a two-step process is employed: (i) electrospinning to generate the fibrous mat, followed by (ii) photo-induced crosslinking to

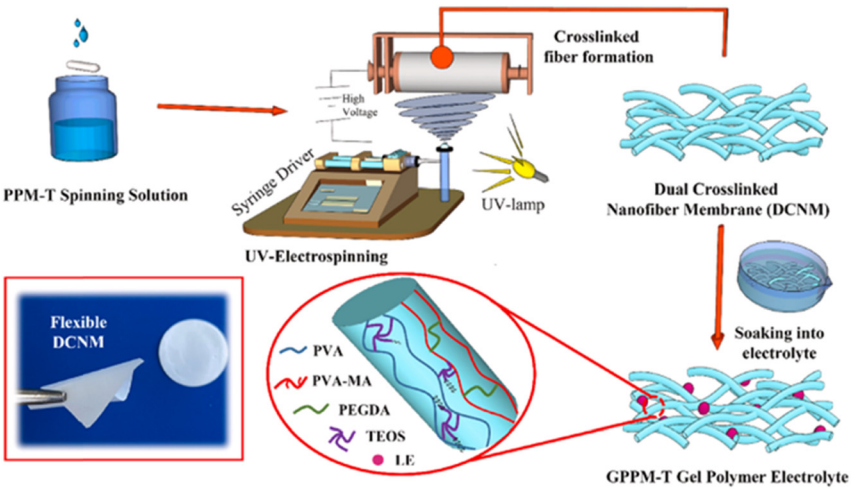

Fig. 10 Dual-crosslinking of electrospun fibers based on UV-photocrosslinking and sol–gel processes: preparation procedure of the dual crosslinked PVA/PVA-MA/TEOS membrane by UV-electrospinning as a matrix for gel polymer electrolyte. Figure reproduced from ref. 69 with permission from Elsevier B.V., Copyright © 2021.

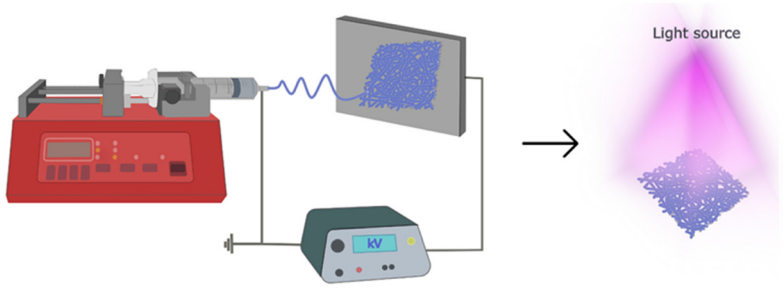

Fig. 11 Schematic of the set-up of the electrospinning process coupled with subsequent light irradiation.

stabilize and functionalize the structure. This approach is most often used with high-molecular-weight polymers that are readily spinnable from solution or melt, but whose as-spun mats may lack adequate resistance to water and humidity or show insufficient mechanical and thermal stability. Nonetheless, several studies also exploit low-molecular-weight photoactive additives incorporated into electrospun mats, which can contribute to network formation or secondary functions upon irradiation.

In general, coupling electrospinning with post-spinning photo-induced crosslinking provides a versatile strategy to introduce covalent networks within and/or between fibers, thereby improving solvent resistance, mechanical integrity, and long-term dimensional stability while largely preserving the nanofibrous morphology. In the following subsections, representative systems are organized by crosslinking chemistry: (meth)acrylate radical systems, thiol–ene click reactions, other radical pathways including photocycloadditions and hydrogen-abstraction strategies, and cationic photopolymerization. The proposed works show that post-spinning photo-induced crosslinking provides a powerful and modular toolbox for stabilizing electrospun mats and imparting advanced mechanical, chemical, and functional properties, further underscoring the strong synergy between electrospinning and photochemistry in soft matter design.

3.1 (Meth)acrylic systems

(Meth)acrylate photocrosslinking is a free-radical process initiated by UV or visible light that converts acrylate/methacrylate functionalities into covalently crosslinked polymer networks. Owing to fast curing kinetics, broad monomer/macromer availability, and highly tunable network properties, (meth)acrylate chemistries dominate photopolymerization and have become a standard toolbox for stabilizing electrospun mats. In electrospinning, (meth)acrylate-functionalized polymers can be spun into fibrous architectures and subsequently cured to yield mechanically robust, solvent-resistant membranes while retaining the high surface area and porosity intrinsic to nanofibrous mats.[71] Acrylic reactivity can be introduced in two main ways: (i) adding low-molecular-weight multifunctional acrylate crosslinkers to the spinning formulation, or (ii) covalently installing (meth)acrylate groups onto polymer backbones to render them intrinsically photo-reactive. Both strategies are widely applied to both synthetic and natural polymers, including poly(ethylene oxide) (PEO), PVA, polysaccharides (*e.g.*, chitosan, hyaluronate, dextran, alginate), proteins (*e.g.*, gelatin, silk fibroin), and

polyesters. (Meth)acrylic photocrosslinking thus represents a versatile platform for the post-spinning stabilization and functional modification of electrospun fibrous mats, enabling systematic tuning of crosslink density, aqueous stability, degradation, and mechanical response.

3.1.1 PEO-based mats. PEO is frequently used in electrospinning (notably in biomedical formulations) thanks to its solubility and chain entanglement, but its high-water solubility and modest mechanical strength often require stabilization. Post-spinning photocrosslinking with multifunctional acrylates has therefore been used to convert PEO mats into water-resistant networks. The group of Vitale introduced multifunctional acrylate crosslinkers into PEO formulations, enabling photocuring after electrospinning. The influence of crosslinker type (*i.e.*, PEGDA or trimethylolpropane triacrylate, TMPTA) and content was systematically investigated, confirming successful network formation. In particular, when TMPTA was used at 25–45 wt%, the resulting PEO membranes exhibited homogeneous fibrous morphology and high resistance to water.[72] Beyond aqueous stability, photocrosslinked PEO/TMPTA mats also showed improved thermal and shape stability, retaining integrity over repeated heating–cooling cycles and exhibiting high latent heat values, demonstrating potential for thermal energy storage applications.[73] More recently, irradiation has been exploited not only to crosslink the PEO/TMPTA matrix but also to synthesize or activate/modify nanofillers *in situ*. In one example, UV exposure enabled simultaneous PEO crosslinking and partial photoreduction of graphene oxide, improving shape stability under heat and solvent exposure and thermal transport in nanocomposite mats.[74] In another study, $AgNO_3$-containing PEO formulations were irradiated to induce the concurrent photo-induced PEO crosslinking and photo-induced synthesis of Ag nanoparticles by photoreduction of Ag^+ ions. Importantly, nanoparticle formation slightly altered fiber morphology but did not prevent acrylate conversion, and the resulting mats combined antibacterial performance with cytocompatibility exhibiting promising potential for wound healing applications.[75] Acrylic-crosslinked PEO networks have also been proposed as functional supports beyond biomedicine: PEO/PEGDA blends were optimized to yield water-stable nanofibrous mats that could host heterogeneous catalysts (Au/Pd on TiO_2), enabling aqueous-phase catalysis while maintaining the fibrous structure.[76]

3.1.2 PVA-based mats. PVA is another readily electrospinnable, water-soluble polymer widely considered for wound dressings and hydrogel-like mats; however, dissolution in aqueous media necessitates post-spinning stabilization. Methacrylated PVA (MPVA) is a common route: increasing methacrylation (degrees of substitution DS 0.01–0.07) reduced hydrophilicity and enabled UV-crosslinked MPVA mats to preserve fibrous morphology in water (with limited swelling at fiber junctions), unlike non-irradiated controls.[77] A complementary strategy combined MPVA with PEGDA and used multistep UV curing to generate stable fibrous hydrogels: ribbon-like fibers ($\sim$1.02 μm) maintained morphology after phosphate buffered saline (PBS) immersion despite pronounced swelling and supported cell viability/adhesion.[78] Beyond biomedical uses, photopolymerization has also been integrated with PVA electrospinning to address separator limitations in lithium-ion batteries: PVA was combined with *N*,*N*-dimethylacrylamide (DMAAm) to form crosslinked hydrogel nanofiber membranes (Fig. 12), where drying protocols (*e.g.*, freeze drying) controlled porosity and electrolyte uptake, delivering high ionic conductivity and thermal stability.[79]

3.1.3 Polysaccharide-based mats. Electrospinning of polysaccharides (*e.g.*, chitosan, hyaluronic acid, dextran, alginate) is inherently challenging due to their rigid molecular backbones, strong intermolecular hydrogen bonding, and limited chain entanglement. These limitations are commonly addressed by blending with carrier polymers (*e.g.*, PEO, PVA) and then "locking"/stabilizing the structure *via* photocrosslinking and/or by directly introducing (meth)acrylate groups. Chitosan (CS), despite its excellent biofunctionality, is a classic example: CS/PVA formulations crosslinked with PEG dimethacrylate yielded mats whose swelling decreased as crosslinker content increased, consistent with higher network density.[80,81] Alternatively, methacrylated chitosan (MACS) blended with PVA could be photocrosslinked and subsequently water-treated to remove PVA, producing stable MACS fibers with a diameter controlled by the MACS/PVA ratio.[82] Related methacrylation approaches have also been developed with scalability in mind: MACS/PEO blends were electrospun and UV-cured to yield markedly

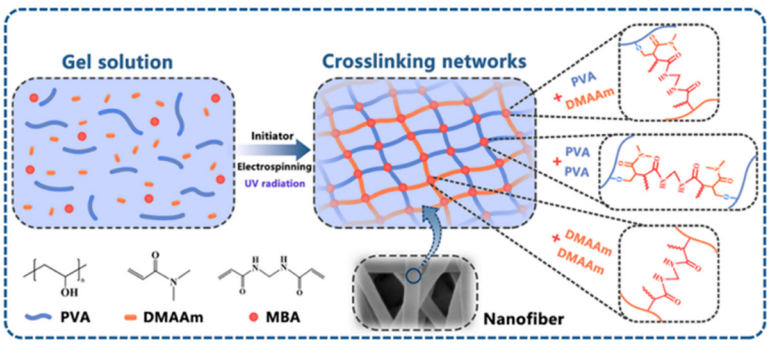

Fig. 12 Photocrosslinked PVA-based mats: schematic diagram of crosslinking mechanism between PVA and DMAAm under UV irradiation. Figure reproduced from ref. 79 with permission from Elsevier B.V., Copyright © 2023.

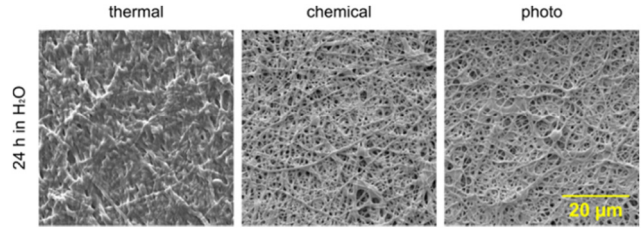

Fig. 13 Comparison among three different crosslinking methods for MACS/PEO mats: SEM images of nanofiber samples crosslinked *via* thermal treatment, chemical crosslinking with glutaraldehyde vapors, and photocrosslinking, after 24 h of water immersion. Figure reproduced from ref. 83 with permission from Springer Nature, Copyright © 2025.

improved aqueous stability, in a workflow positioned for continuous production. This very recent work compared different crosslinking methods (Fig. 13) and showed that photocrosslinked nanofibers exhibited greater stability than those crosslinked thermally and perform comparably to chemically crosslinked samples in terms of structural integrity.[83]

Hyaluronic acid (HA), a naturally occurring, highly hydrophilic glycosaminoglycan of the extracellular matrix whose excellent biocompatibility and chemical tunability make it an attractive candidate for electrospinning into bioactive nanofibrous scaffolds, has likewise been processed *via* carrier-assisted electrospinning and stabilized by UV chemistry. In one approach, HA was electrospun with PVA as carrier (PVA/HA = 75/25), and the resulting mats were UV-crosslinked using maleic anhydride (5–15 wt%) as crosslinker. Increasing the crosslinker content led to a reduction in fiber diameter and significantly improved the structural stability of the mats in aqueous environments.[84] In a related strategy, methacrylated HA further enabled photocrosslinking spatial control: after electrospinning methacrylated HA with PEO as a template, irradiation through photomasks produced localized polymerization and macroscopic channels throughout the scaffold, generating a multiscale porous architecture (Fig. 14) that helped mitigate the limited cell infiltration typical of dense electrospun mats.[85]

Dextran and alginate provide additional examples of how acrylic functionalization expands polysaccharide processability. For instance, dextran–maleic anhydride (Dex-Ma), blended with gelatin at contents ranging from 0 to 30%, was successfully electrospun and photocrosslinked to obtain fibrous membranes for tissue engineering. Increasing Dex-Ma content resulted in progressively thinner fibers and, at 30% Dex-Ma, led to reduced water uptake and a higher elastic modulus while preserving cytocompatibility.[86] In a related approach, methacrylated alginate derivatives and methacrylated heparin were electrospun with PEO (1 : 1) and subsequently photocrosslinked. After removal of the PEO carrier to improve cell accessibility, the resulting mats retained their fibrous morphology over short culture periods and underwent gradual degradation over several weeks, while the presence of biofunctional motifs promoted enhanced cell interactions and controlled release behavior.[87]

3.1.4 Protein-based mats. Protein-based electrospun mats are particularly attractive for biomimetic applications but generally require crosslinking to prevent rapid dissolution and to enable control over mechanical properties and degradation behavior.[88] Methacrylated gelatin (GelMA), a denatured collagen derivative, is among the most widely used examples: it can be readily electrospun and subsequently UV-cured to yield stable fibrous hydrogels. GelMA mats have been employed as antibiotic-releasing membranes (*e.g.*, azithromycin-loaded systems) with controlled degradation and release kinetics,[89] and more broadly as mechanically reinforced fibrous scaffolds through blending with synthetic polymers and/or fillers.[90–94] These strategies have enabled fine tuning of stiffness, extensibility, and cellular response across a wide range of tissue-specific applications.[95] More recently, GelMA has been combined with elastin-like peptides (ELPs) to fabricate biomimetic, suturable, and extensible electrospun scaffolds (Fig. 15). By optimizing composition, a 5 : 5% (w/v) ELP/GelMA formulation was identified as providing the best balance of mechanical compliance, degradation rate, biocompatibility, and cell proliferation, closely matching the requirements of lower urinary tract tissues.[96]

Beyond improving intrinsic fiber stability, (meth)acrylic photochemistry also enables hierarchical structure of electrospun mats, including core–shell, multilayer, and composite architectures with spatially separated functions. Coaxial electrospinning, for example, has been used to produce core–shell fibers comprising a PCL core and a photocrosslinked GelMA shell for vascular tissue engineering applications.[97] Similarly,

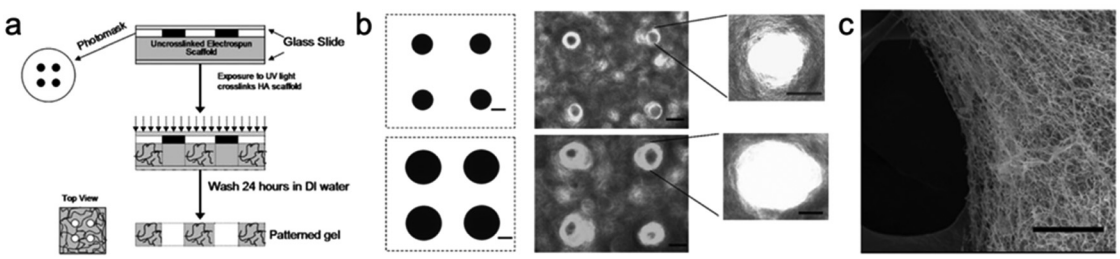

Fig. 14 Combination of electrospinning with photopatterning to create multiscale porous scaffolds: (a) schematic representation of the technique to photopattern macro-channels into electrospun scaffold; (b) light micrographs of photomasks and top-view of patterned HA scaffolds (scale bars = 100 μm); and (c) SEM image of electrospun scaffold structure after unreacted HA and PEO removal (scale bar = 50 micrometers). Figure reproduced from ref. 85 with permission from Wiley-VCH, Copyright © 2010.

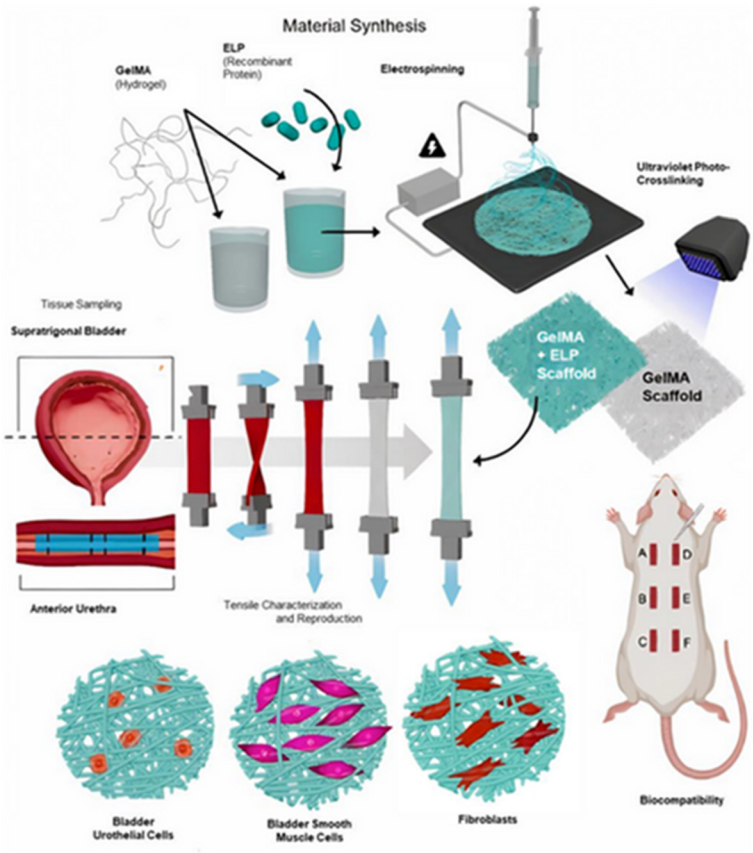

Fig. 15 Schematic representation of the synthesis and evaluation of ELP/GelMA fibrous scaffolds: the process includes electrospinning, photocrosslinking, mechanical characterization, *in vitro* cell seeding, and *in vivo* biocompatibility assessment *via* subcutaneous implantation in a rat model. Figure reproduced from ref. 96 with permission from Wiley-VCH, Copyright © 2025.

poly(lactic-*co*-glycolic acid) (PLGA)/gelatin methacrylamide core–shell fibers benefited from crosslinking the shell in gelatin solution, improving mechanical and biological performance.[98] Another interesting structure was presented by the group of Ferreira, who functionalized both gelatin and chitosan with methacrylic functions (GelMA and ChMA), and integrated them into a bilayer wound-dressing membrane. The mesh was fabricated by sequential electrospinning of a hydrophobic PCL/PLA top layer (protective barrier) followed by a GelMA/ChMA underlying layer, then UV irradiation to crosslink the bioactive phase. The barrier layer limited external water infiltration, whereas the GelMA/ChMA layer provided high wettability and an ECM-like morphology supportive of cell proliferation. After photocrosslinking, the GelMA/ChMA layer showed minimal mass loss (~6%), while non-crosslinked meshes dissolved completely.[99]

Methacrylated silk fibroin systems further highlight the multifunctionality achievable through the combination of electrospinning and photocrosslinking. Depending on formulation and secondary interactions (*e.g.*, metal coordination), these systems have supported antibacterial activity, angiogenic and osteogenic responses, controlled drug release, and regenerative functions.[100–102]

Finally, photocrosslinking has also been extended to plant-derived proteins. Although soy protein isolate (SPI) shows promise for biomedical, food, and filtration applications, its electrospinnability and stability under physiological conditions are limited. Methacrylation of SPI to obtain a photo-crosslinkable derivative, followed by electrospinning with PEO as a carrier and UV curing, significantly improved both processability and aqueous stability compared to unmodified SPI.[103]

3.1.5 Polyester-derived acrylic systems. Acrylated polyesters have also been used to obtain mechanically reinforced mats through post-spinning photo-induced curing. Ye *et al.* synthesized acrylate-terminated random copolyesters of poly(ε-caprolactone-*co*-L-lactide) (PCLA) and achieved efficient photoinitiator-free UV crosslinking. The tensile strength of the resulting fibrous membranes increased with irradiation time, from approximately 13 to 21 MPa, while early-stage degradation was significantly reduced, enabling preservation of mechanical integrity for at least one month.[104] In a related strategy, polyester-based porous ultrafine fibers were fabricated using a phase-separation-assisted approach. Blends of unsaturated polyester macromonomer (UPM) and poly(3-hydroxybutyrate-*co*-3-hydroxyvalerate) (PHBV) were electrospun, with PHBV serving as an electrospinnable carrier to compensate for the low viscosity and molecular weight of UPM. The resulting fibers exhibited a cylindrical morphology with average diameters ranging from 0.5 to 20 μm. After electrospinning, UPM was photocrosslinked under UV irradiation,

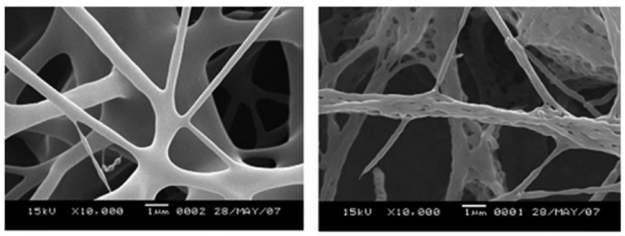

Fig. 16 Porous photocrosslinked nanofibrous structure obtained by phase separation and selective solvent extraction: SEM images of UPM/PHBV (4/1) after 1 h (a) and 24 h (b) washing step with chloroform. Figure reproduced from ref. 105 with permission from Wiley Periodicals Inc., Copyright © 2009.

and the membranes were subsequently subjected to selective solvent extraction (*e.g.*, chloroform). Due to the immiscibility of UPM and PHBV, phase separation occurred during fiber formation, and removal of PHBV generated a porous nanofibrous structure (Fig. 16).[105] For higher throughput, free surface electrospinning (FSES) (*i.e.*, process in which jets originate from the free surface of a polymer solution under a high electric field rather than from a needle) has been combined with UV curing to produce scalable nanofibrous membranes. Using this technique with aqueous solutions of vinylbenzylated gelatin (gelatin-4VBC) and PCL dimethacrylate (PCL–DMA), UV curing created a covalently integrated co-network; varying the gelatin-4VBC/PCL–DMA ratio and photoinitiator concentration enabled tuning of crosslinking density, wettability, and degradation behavior, with PCL–DMA acting as a hydrophobic degradable crosslinker that also mitigated steric hindrance during curing.[106]

Taken together, these studies demonstrate that (meth)acrylate post-spinning photocrosslinking of polymeric systems provides a general and highly adaptable route to stabilize water-soluble electrospun polymers, while preserving nanofibrous morphology and enabling fine control over mechanical properties, degradation, and biointeractions.

3.1.6 Macromers and liquid-crystalline building blocks. Even in post-spinning curing approaches, limited segmental mobility within highly entangled polymer chains can restrict crosslinking efficiency, motivating the use of more reactive low-molecular-weight (meth)acrylic species or oligomers. Macromers and prepolymers offer an effective intermediate strategy between small monomers and high-molecular-weight polymers, combining sufficient processability for electrospinning with a high density of photoreactive functional groups. A wide range of acrylic-based macromers has been synthesized and electrospun either alone,[107] with PEO as a carrier,[108,109] or blended with gelatin,[110] yielding photo-crosslinkable nanofibers suitable for hydrogel formation and tissue-regeneration scaffolds. Crucially, rational molecular design enables fine control over photoreactivity, crosslinking efficiency, fiber morphology, solubility, and mechanical performance, making macromer-based systems highly versatile platforms for integrating electrospinning with photochemistry.

A distinct yet related class is represented by reactive mesogens (RMs), liquid-crystalline monomers bearing polymerizable terminal groups and exhibiting intrinsic molecular alignment in their mesophases. Upon UV irradiation, these monomers undergo photopolymerization, permanently fixing the ordered structure into oriented polymer networks. This self-organizing behavior offers a unique route to high-performance electrospun fibers. In this context, Yao *et al.* combined acrylate-functional RMs with polyamide 6 (PA6) or PMMA, obtaining improved mechanical properties at RM contents between 20 and 33 wt%, while higher loadings were detrimental.[111] A closely related class involves light-responsive liquid crystal elastomer (LCE) fibers and yarns fabricated by electrospinning followed by photocrosslinking. In advanced designs incorporating photothermal additives such as gold nanorods (AuNRs), electrospinning was combined with molecular synthesis and a two-step crosslinking strategy (Fig. 17). During solution preparation, the acrylic liquid-crystal monomer (RM257) and polymerizable AuNRs underwent an initial Michael addition with a thiol-containing chain extender, forming short liquid-crystalline oligomers that were electrospun and collected as aligned yarns using a funnel-shaped collector. Subsequent UV-induced acrylic crosslinking and roller drafting fixed molecular orientation within the fibers. Owing to the interconnected "spider-web-like" fiber architecture, high molecular alignment, and robust covalent bonding at the organic–inorganic interface, the resulting LCE yarns exhibited large, reversible actuation strains

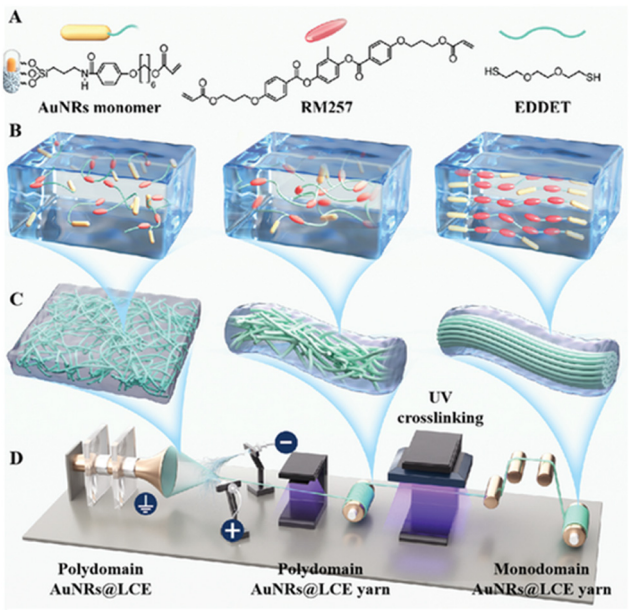

Fig. 17 Light-driven liquid crystal elastomer (LCE) active yarn fabricated by electrospinning and subsequent photocrosslinking strategies: (A) molecular structure of monomers and chain extenders; (B) and (C) schematic diagram of internal molecular chain and fibers network structure changes in the electrospun yarn soft actuator; (D) schematic diagram of the preparation process of the AuNRs@LCE active yarn soft actuator. Figure reproduced from ref. 112 with permission from Wiley-VCH, Copyright © 2024.

(≈81%) and stable light-driven shape-morphing behavior under varying irradiation intensities.[112]

Together, macromers and liquid-crystalline building blocks illustrate how molecular design and photochemistry can be leveraged to overcome mobility limitations in electrospun systems, enabling hierarchical organization, efficient network formation, and emergent mechanical and functional properties unique to nanofibrous soft matter.

3.2 Thiol–ene systems

The thiol–ene "click" reaction is a hydrothiolation process between thiol groups and carbon–carbon double bonds that combines the hallmark features of click chemistry (*i.e.*, high efficiency, selectivity, and orthogonality) with the advantages of photopolymerization. Upon light activation, thiol–ene reactions proceed through a radical-mediated step-growth mechanism, leading to uniform network formation with reduced oxygen inhibition and low polymerization shrinkage.[113] These features make thiol–ene chemistry particularly well suited for coupling with electrospinning to fabricate crosslinked nanofibrous membranes with controlled morphology and functionality. By selecting the thiol crosslinker and tuning the thiol-to-ene ratio, both the structural and functional properties of electrospun mats can be precisely tailored.

A representative example is provided by Sharma *et al.*, who combined electrospinning with thiol–ene crosslinking to fabricate fibrous PEG hydrogels that better mimic the fibrous architecture and biological microenvironment of native tissues compared to bulk hydrogels. In this approach, four-arm PEG-norbornene (PEG-NB) was electrospun using PEO as a sacrificial carrier and subsequently crosslinked with multifunctional thiols. The influence of different thiol crosslinkers (2,2′-(ethylenedioxy)diethanethiol EDT, pentaerythritol tetrakis(3-mercaptopropionate) PETMP, and poly(ethylene glycol) dithiol PEGDT) was systematically investigated. The molecular weight and functionality of the thiol crosslinker affected solution viscosity and fiber diameter, which ranged from 0.5 to 3.5 mm in dry state, with PEGDT yielding the largest fibers. The mechanical properties of the fibrous hydrogels were governed by UV exposure time, solvent conditions, and crosslinker type, with longer irradiation increasing shear modulus. PETMP-crosslinked fibers exhibited the highest shear modulus (∼2.7 kPa) after 30 min UV exposure, consistent with its higher thiol functionality.[114] Thiol–norbornene photochemistry has also enabled elastomeric and bioactive hydrogel fibers based on synthetic polyesters. Norbornene-functionalized PGS-*co*-PEG macromers were electrospun with PEO as a carrier and subsequently crosslinked with dithiols to form fibrous hydrogels. This approach overcame the limitations of conventional thermally cured PGS and yielded cytocompatibility scaffolds with tunable elasticity, highlighting the versatility of thiol–ene chemistry for fabricating fibrous elastomers.[115] In vascular tissue engineering, PEG-NB has been used to create hybrid electrospun grafts with tunable mechanics and porosity. Core–sheath fibers comprising a PEG-NB shell and hydrophobic cores (PCL or PLCL) were photocrosslinked *via* thiol–ene reactions (with PEG-thiol crosslinkers), and post-processing by freeze-drying further enhanced porosity and tensile properties. The choice of core polymer and processing route enabled independent control of stiffness, degradation rate, and cell infiltration, demonstrating the adaptability of thiol–ene crosslinking for vascular graft design.[116] NB-based chemistry has also been applied to polypeptide systems. Norbornene-modified polysuccinimide (PSI-NB) was electrospun and crosslinked with multifunctional thiols to yield stable fiber networks that were subsequently hydrolyzed to poly(aspartic acid) (pAsp) (Fig. 18). Although hydrolysis induced fiber swelling, the photocrosslinked structure remained intact, illustrating how thiol–ene networks can stabilize otherwise water-soluble fibrous assemblies.[117]

Functional bioactive fibers have further been realized using thiol–ene reactions. Methacrylated HA combined with PEG-thiol crosslinkers enabled the fabrication of biodegradable nitric oxide (NO)-releasing nanofibers for wound healing. By tuning HA concentration and NO-donor content, fiber diameter, NO payload, and release duration were precisely controlled, while maintaining cytocompatibility.[118]

Beyond hydrogels, thiol–ene crosslinking has been exploited to stabilize elastomeric and rubbery electrospun mats. Vitale *et al.* demonstrated morphology-controllable styrene–butadiene rubber (SBR) nanofibers crosslinked *via* thiol–ene reactions. Different process parameters (*e.g.*, flow rate, time between the electrospinning and the irradiation) were demonstrated to be efficient in controlling the fiber diameter up to the

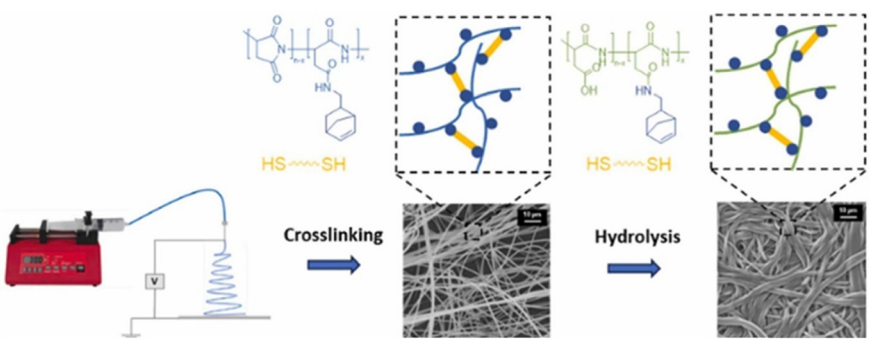

Fig. 18 Photo-crosslinked poly(aspartic acid) fiber networks *via* electrospinning and subsequent alkaline hydrolysis. Figure reproduced from ref. 117 with permission from Elsevier Ltd., Copyright © 2024.

nanometer range and of the membrane porosity. Crosslinking prevented cold flow and provided long-term dimensional stability. Moreover, adjusting the thiol-to-vinyl molar ratio and the irradiation dose enabled precise control over the density of residual functional groups available for post-functionalization.[119] In a subsequent study aligned with sustainability principles, SBR-based electrospun membranes were prepared from aqueous SBR latex in water rather than organic solvents, and crosslinked with thiols. PEO was used as a template polymer to make the suspension electrospinnable, and was then removed after electrospinning and UV irradiation by water washing, yielding raspberry-like fibers composed solely of SBR nanoparticles (Fig. 19). The formation of a three-dimensional crosslinked network, which imparted excellent structural stability after water treatment and enhanced thermal performance, was confirmed. Tuning the composition of the electrospinning suspension allowed to finely control the chemical composition, morphology, water solubility, and thermal properties of the nanofibrous membranes.[120] Thiol–ene chemistry has also been applied to polyester systems, including elastic polyurethane fibers with shape-memory behavior[121] and copolyesters based on alkyne-functionalized and thiol-bearing moieties with biodegradable grafts capable of sustained hydrogen sulfide release to promote endothelial cell growth.[122]

Overall, thiol–ene photochemistry provides a robust and versatile platform for the photocrosslinking of electrospun mats, enabling efficient network formation under mild conditions and offering fine control over fiber morphology, mechanical properties, and surface functionality.

3.3 Other radical systems

In addition to (meth)acrylate and thiol–ene chemistry, several other radical-mediated photocrosslinking mechanisms have been employed to stabilize electrospun mats, each offering distinct advantages in terms of efficiency, stability, and functional control. For instance, nitrene-based crosslinking relies on highly reactive species generated from arylazide groups under UV irradiation. Christ and Menzel functionalized fungal chitosan with photoreactive arylazides (CS–Az) and blended it with ultrahigh-molecular-weight PEO to obtain smooth, defect-free fibers. Upon irradiation, arylazides generated nitrenes that can work as either diradical (triplet state) or as electrophile (singlet state) by bimolecular insertion into C–H or N–H bonds of adjacent chains, producing a water-stable crosslinked network (Fig. 20).

Fiber morphology was mainly governed by PEO content and solvent volume, highlighting the importance of formulation design.[123]

Photocycloaddition reactions, particularly [2+2] cycloadditions of cinnamate or styryl groups, constitute another widely used strategy. For example, methylene cinnamate pendants were introduced into polystyrene, enabling photoinitiator-free UV crosslinking through cyclobutane formation. The resulting fibers ($\approx$350 nm) exhibited excellent solvent resistance and reversible crosslinking under deep-UV exposure ($<$260 nm),[124] although such high-energy irradiation may limit penetration depth and raise photodegradation concerns in thicker assemblies. Similar reversible stabilization was achieved in an interesting work, where highly hydrophilic poly(2-ethyl-2-oxazoline) (PEtOx) nanofibers functionalized with cinnamoyl moieties were dimerized under UVB irradiation, while UVC exposure enabled controlled disintegration.[125]

A closely related family relies on styrylpyridinium (SbQ) groups, which undergo [2+2] cycloaddition under UV light and have been extensively used to stabilize PVA. PVA–SbQ nanofibers retained morphology and exhibited low mass loss upon prolonged water immersion.[126] Moreover, irradiation with linearly polarized light enabled directional crosslinking, yielding anisotropic, dichroic fibrous membranes.[127,128] Related photocycloaddition strategies based on thienyl acrylate substituents yielded water-resistant PVA fibers with reduced diameters (100–200 nm).[129] This photocrosslinking strategy has recently been translated to scalable, needle-free electrospinning (production $\approx$15 g h^{-1}; Fig. 21) for high-flux water purification

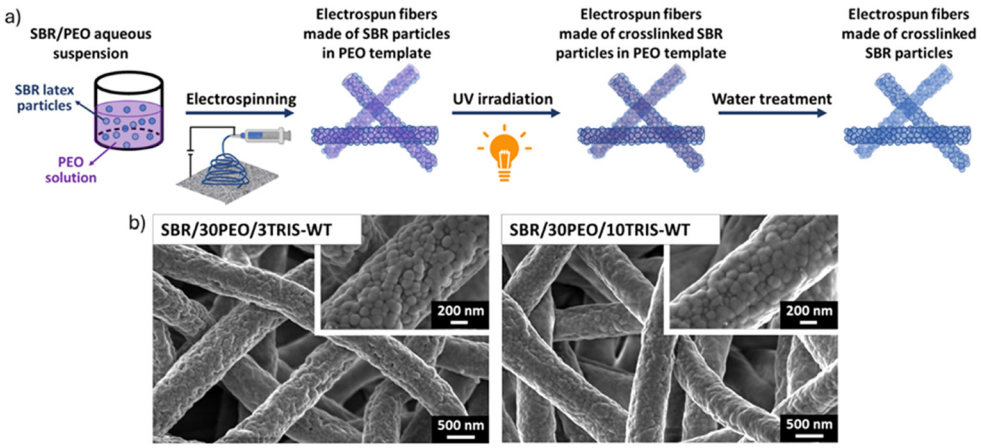

Fig. 19 SBR fibrous membranes by latex electrospinning and thiol–ene photocrosslinking: (a) schematic illustration of the process, and (b) morphology of the photo-crosslinked electrospun membranes after water treatment for PEO removal. Figure adapted from ref. 120 with permission from Springer, Copyright © 2024.

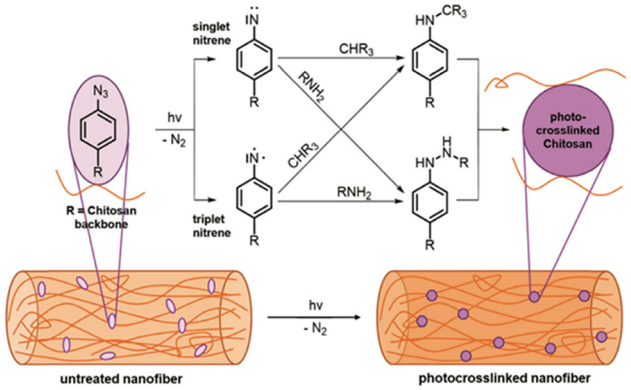

Fig. 20 Photocrosslinking mechanism of highly modified CS-Az. Figure reproduced from ref. 123 with permission from Wiley-VCH, Copyright © 2022.

membranes, where double-bond addition cyclopolymerization-based photocrosslinking controlled swelling and pore structure while maintaining high permeability and high rejection efficiency.[130] Beyond membranes, SbQ photochemistry has also enabled nanofiber-based microparticles: electrospinning of PVA–SbQ followed by photopatterning generated detachable, shape-defined fibrous microstructures that were collected in water and functionalized with Ag nanoparticles as capture substrates for surface-enhanced Raman spectroscopy (SERS)-based multiplex immunoassays.[131]

While these reversible photochemical motifs enable dynamic behavior in nanofibrous systems, their practical implementation in thick or multilayered architectures may be constrained by light-penetration limitations, particularly in highly scattering fibrous mats where photon flux decays rapidly with depth.

Radical pathways based on hydrogen abstraction and recombination provide an alternative to photocycloaddition. Benzophenone-functionalized poly(2-ethyl-2-oxazoline) underwent UV-induced crosslinking *via* hydrogen abstraction and radical coupling; among different irradiation strategies, post-spinning curing proved most effective in achieving water-stable membranes.[132] Similarly, Kianfar *et al.* stabilized chitosan-containing electrospun mats using PEO as a carrier and benzophenone as a hydrogen-abstraction photoinitiator, avoiding additional crosslinkers or polymer functionalization. Despite partial chitosan degradation at high doses, the membranes showed improved thermal and water resistance while preserving biocompatibility.[133]

Beyond amorphous polymers, photocrosslinking of ordered and functional systems has also been demonstrated. Liquid-crystal elastomer fibers with uniformly aligned nematic directors were produced by electrospinning photoactive main-chain polymers followed by UV curing under orientation fields.[134] In parallel, photo-responsive conjugated polymers such as polydiacetylene (PCDA) have been incorporated into electrospun fibers for sensing applications. It was shown that embedding PCDA in PEO or PU matrices enabled bead-free fibers with preserved conjugation and colorimetric response to bacteria and pH, provided that solution viscosity and composition were carefully controlled.[135,136]

Overall, these examples demonstrate that grouping photocrosslinking strategies by reaction mechanism (*e.g.*, nitrene insertion, photocycloaddition, radical recombination) provides a useful framework for rationally designing electrospun mats with tailored stability, functionality, and responsiveness, further highlighting the strong synergy between electrospinning and photochemistry.

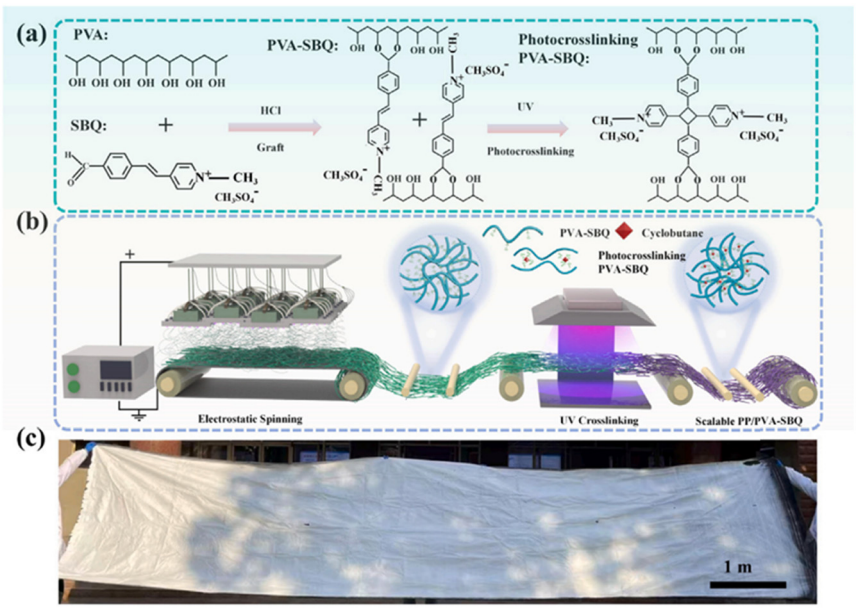

Fig. 21 Scalable and durable electrospun photocrosslinked PVA-SbQ nanofibers-based membranes: (a) schematic diagram of the changes of functional groups in the molecular chain; (b) schematic of the preparation process of the nanofibrous membranes; (c) physical image of the electrospun membrane. Figure reproduced from ref. 130 with permission from Elsevier B.V., Copyright © 2025.

3.4 Cationic systems

Cationic photopolymerization is a light-initiated process in which strong acids are generated from onium salts to initiate polymerization of monomers such as epoxides, vinyl ethers, and related functionalities. This mechanism offers several advantages over free-radical photopolymerization, including negligible oxygen inhibition, low volumetric shrinkage, and the formation of mechanically robust networks. Moreover, the monomers employed in cationic systems are often less toxic than the acrylate and methacrylate monomers commonly used in radical photopolymerization. A distinctive feature of cationic photopolymerization is its ability to proceed even after the light source is removed (dark curing), owing to the relatively long lifetimes of the photogenerated acidic species.[137] In highly scattering fibrous systems, this post-irradiation propagation can partially compensate for limited photon penetration, promoting improved cure depth compared to radical systems. Nevertheless, the initial spatial distribution of acid generation still depends on the local light intensity, and therefore remains influenced by the scattering coefficient and optical density of the mat.

The advantageous features of cationic mechanism have been successfully exploited in electrospinning. Iregui *et al.* fabricated shape-memory fibers by electrospinning blends of bisphenol A diglycidyl ether (DGEBA), high-molecular-weight PCL, and iodonium salt, followed by UV curing. The resulting membranes exhibited excellent shape-memory performance, with shape-fixity ratios of 95–99% and shape-recovery ratios of 88–100%.[138] Electrospun fibers exhibited superior fixity and recovery, attributed to a highly anisotropic ''shish kebab'' crystalline morphology in which oriented PCL chains were covalently linked to the epoxy network. This unique morphology conferred exceptional solvent resistance, shape-memory properties, and enabled potential applications in unconventional fields such as chloroform sensing.[139]

Cationic photopolymerization has also been integrated with electrospinning and photolithography to create functional fibrous architectures. Electrospun membranes were fabricated from SU-8, an epoxy-based negative photoresist, and subsequently patterned using conventional photolithography with controlled UV exposure through photomasks of varying periodicity. After patterning, a thin silver layer was deposited by thermal evaporation to produce SERS substrates. The resulting membranes consisted of uniform fibers with average diameters of approximately 200 nm and featured well-defined micropatterns (100–400 μm). The homogeneous fibrous structure provided highly reproducible SERS performance, with enhancement factors on the order of 10^8 for Rhodamine 6G detection.[140]

4. Photo-induced grafting/surface modification of electrospun mats

Beyond bulk crosslinking, photo-induced reactions offer powerful routes for the surface modification and functionalization of electrospun mats, enabling the fabrication of coated fibers, core–shell architectures, and multilayered systems with tailored interfacial properties. Owing to the spatial and temporal control afforded by light, photografting and photocuring are particularly well suited for introducing bioactivity, tunable wettability, or stimulus responsiveness while preserving the intrinsic fibrous morphology. Because electrospun mats are dominated by interfacial area rather than bulk volume, surface chemistry plays a disproportionate role in governing their macroscopic behavior, making photo-induced grafting particularly impactful in these soft, high-surface-area systems.

One common strategy consists of coating electrospun fibers with a photocrosslinked hydrogel layer. For example, cellulose acetate nanofibers loaded with ibuprofen were coated with a poly(acrylamide) hydrogel formed by UV photopolymerization of acrylamide, yielding drug-delivery systems with sustained release profiles and excellent cytocompatibility. Compared to uncoated fibers, the hydrogel shell suppressed burst release and enabled near-complete drug delivery at higher loadings.[141] Similarly, temperature-responsive fibers were fabricated by electrospinning PCL fibers followed by coating through *in situ* UV photopolymerization of poly(N-isopropylacrylamide) (PNIPAM) layer. The PNIPAM layer enabled temperature-dependent wettability and antibiotic release, resulting in effective antibacterial activity against both *E. coli* and *S. aureus*.[142] Photocrosslinked gelatin-based coatings have also been applied to electrospun PCL scaffolds for vascular tissue engineering, where GelMA, PEG acrylate, and PEG diacrylate hydrogels improved hemocompatibility and endothelial cell interactions.[143]

Photo-induced surface grafting has further enabled direct immobilization of bioactive macromolecules onto fibrous substrates. In one example, azidobenzoic-acid-modified gelatin was photochemically grafted onto PHBV/PEO electrospun mats without additional crosslinkers, significantly enhancing cell adhesion and proliferation relative to ungrafted controls. Although grafting increased fiber diameter and slightly reduced porosity and mechanical strength, optimized formulations showed balanced morphology, permeability, and mechanical performance suitable for artificial skin scaffolds.[144]

Beyond biomedical coatings, photografting has been recently exploited for wearable and sensing platforms. Patterned polystyrene-*block*-polybutadiene-*block*-polystyrene (SBS) nanofibers fabricated using structured collectors were rendered hydrophilic through benzophenone-initiated photografting of PEGMA (Fig. 22), enabling uniform hydrogel integration. Subsequent selective photopolymerization of PEGDA hydrogels containing enzymatic and pH-responsive reagents produced power-free, colorimetric sweat sensors capable of real-time glucose and pH monitoring, with demonstrated on-body performance and biocompatibility. The photografted PEGMA layer was essential for stable hydrogel anchoring, enhanced wettability, and reliable analyte diffusion.[145]

These coating-based approaches illustrate how photo-induced grafting can selectively modify surface chemistry without perturbing bulk fiber structure, enabling independent optimization of interfacial and mechanical properties, and

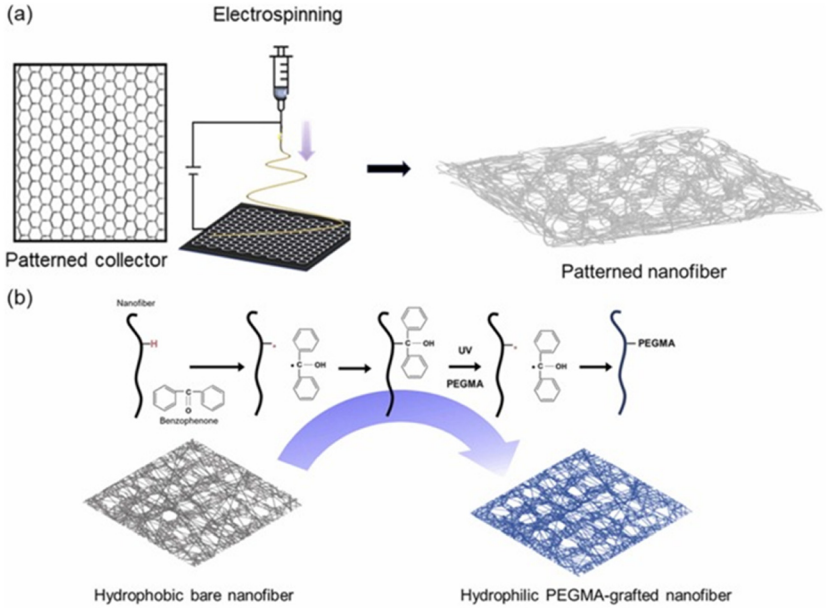

Fig. 22 Schematic illustration of the fabrication and surface modification of patterned SBS nanofibers: (a) electrospinning using a patterned collector to create structured nanofibers with controlled alignment; (b) surface modification of SBS nanofibers *via* PEGMA grafting using benzophenone-initiated UV polymerization to enhance hydrophilicity. Figure reproduced from ref. 145 with permission from Elsevier B.V., Copyright © 2025.

allowing relatively thin grafted layers to dictate wetting, bio-interaction, and transport behavior of the entire fibrous mat.

Photo-induced grafting has also been exploited to create core–shell nanofibers and polymer brush architectures. In one example, fluorinated photoinitiators preferentially migrated to the fiber surface during electrospinning of PAN, enabling surface-initiated photopolymerization of acrylate monomers and the formation of functional polymer shells under UV irradiation.[146] pH-sensitive drug-delivery fibers were fabricated using a similar approach, where PLA-based core fibers loaded with combretastatin A4 were coated with UV-polymerized acrylic shells, yielding controlled drug release under acidic conditions.[147]

Even more complex architectures can be achieved through photo-assisted multilayer fabrication. Bilayer and trilayer nanofibrous membranes with asymmetric wettability and pore gradients were produced by combining electrospinning of PU/PEGDA blends with subsequent PEGDA photocuring. By controlling UV irradiation time and coating thickness, directional moisture transport was achieved, enabling efficient sweat management in advanced textile systems.[148,149]

Photo-induced grafting is particularly effective for tailoring surface chemistry, wettability, and biological interactions. Extensive work by Ramesh and co-workers demonstrated how photografting hydrophilic, zwitterionic, or amino-acid-based moieties onto electrospun poly(ethylene-*co*-vinyl alcohol) (EVAL) fibers modulated wettability and blood compatibility. Grafting of 2-hydroxyethyl acrylate, sulfobetaine methacrylates, or glycine enabled systematic control over leukocyte adhesion, red blood cell recovery, and hemolysis, highlighting the complex interplay between surface hydration, charge, and blood–material interactions.[150–152] Beyond hemocompatibility, photografting has been applied to immobilize therapeutic biomolecules on electrospun scaffolds. Perfluorophenyl azide bearing a *N*-hydroxysuccinimide (PFPA-NHS) active ester group enabled UV-initiated covalent attachment of proteins and enzymes to PCL fibers while preserving biological activity, offering sustained presentation of bioactive cues for regenerative medicine and photodynamic therapy.[153]

Photochemical surface modification has also enabled multifunctional materials with specific surface properties for antimicrobial and environmental applications. Poly(methacrylic acid) brushes were photografted onto PHBV fibers and used to complex *in situ* photogenerated silver nanoparticles, yielding scaffolds with strong antibacterial activity against *S. aureus* and *E. coli*.[154] Selective photografting was further used to fabricate asymmetric PLA/PVA meshes with controlled moisture transport and high cell viability for wound-dressing applications.[155] In another example, hydrophobic/oleophilic rubber nanofibrous membranes were fabricated *via* suspension electrospinning of SBR followed by photo-induced crosslinking and thiol–ene grafting of vinyl-terminated PDMS (Fig. 23). The resulting membranes exhibited stable hydrophobicity, strong oleophilicity, and excellent oil–water separation efficiency ($>99\%$) with high flux, underscoring their potential for oily wastewater remediation.[156]

Overall, these studies demonstrate that photo-induced grafting transforms electrospun mats into modular platforms, where surface functionality, responsiveness, and interfacial interactions can be programmed independently from fiber formation.

Finally, photografting strategies have been extended to stimuli-responsive and energy-storage systems. Hierarchical polystyrene fibrous membranes grafted with pH-responsive and fluorinated acrylates exhibited switchable wettability and

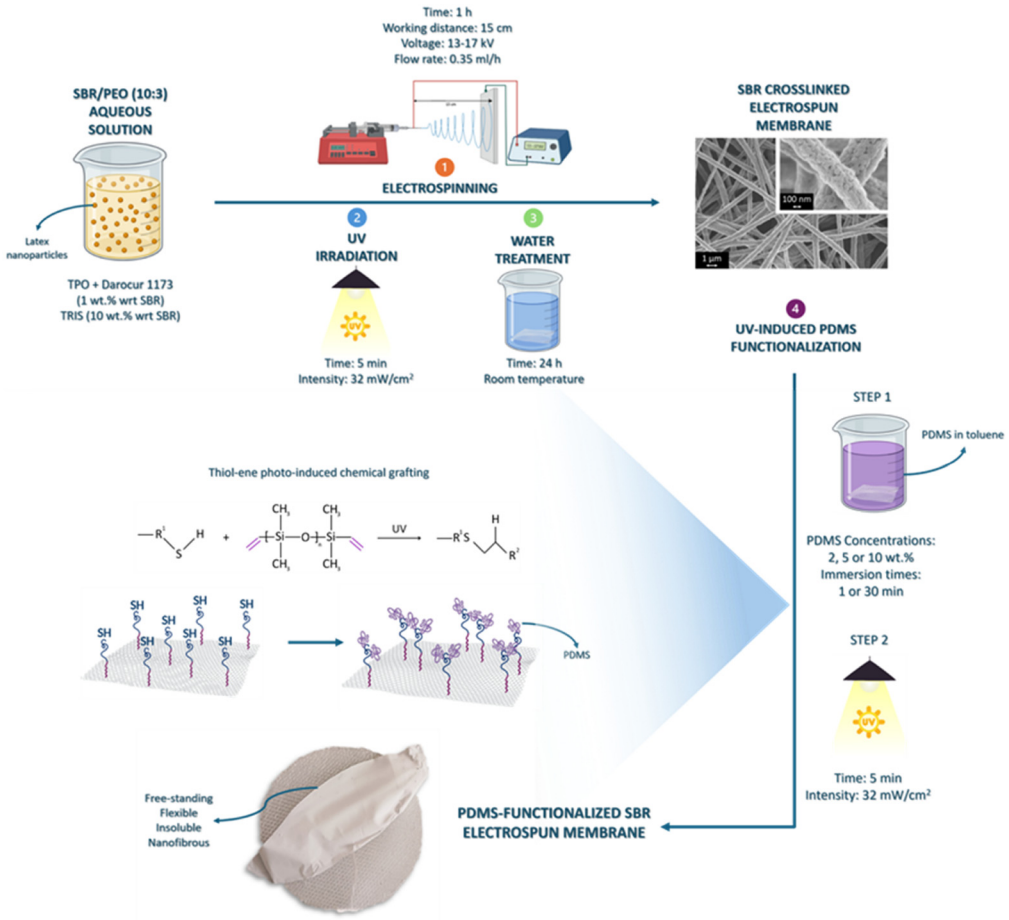

Fig. 23 Scheme of the process to prepare PDMS-grafted electrospun rubber membranes: electrospinning of SBR/PEO suspension, irradiation to promote the photo-induced crosslinking, water treatment to remove PEO template, and photo-induced functionalization with vinyl terminated PDMS. The thiol–ene grafting reaction is also reported. Figure reproduced from ref. 156 with permission from Elsevier B.V., Copyright © 2025.

enabled gravity-driven oil–water separation with high efficiency.[157] In parallel, composite polymer electrolytes were fabricated by electrospinning poly(vinylidene fluoride-*co*-hexafluoropropylene) (PVDF-HFP) and PAN hybrid fibers loaded with metal–organic framework particles, followed by UV-initiated polymerization of a liquid precursor. The resulting interconnected 3D fibrous networks enabled continuous Na^+ transport, high ionic conductivity, and excellent electrochemical performance in quasi-solid-state sodium batteries.[158]

In conclusion, photo-induced grafting and surface modification provide exceptional versatility for engineering electrospun mats with controlled interfacial chemistry, hierarchical architectures, and application-specific functionalities. By decoupling bulk fiber formation from surface functionalization, these strategies greatly expand the design space of electrospun materials for biomedical, environmental, and smart-textile applications.

5. Conclusions and perspectives

The coupling of electrospinning with photo-induced processes has emerged as a powerful and versatile strategy for the design of advanced nanofibrous polymeric materials. As illustrated throughout this review, light-driven polymerization, crosslinking, and grafting reactions provide effective solutions to several intrinsic limitations of conventional electrospinning, including insufficient mechanical robustness, poor resistance to water or solvents, and limited control over functionality. By enabling *in situ* or post-spinning network formation under controlled light-mediated conditions, photochemistry expands both the materials palette and the architectural complexity accessible through electrospinning.

From a materials perspective, the integration of photo-induced reactions has significantly broadened the range of processable systems, encompassing low-molecular-weight monomers and oligomers, macromers, high-performance polymers, natural polymers, and hybrid organic–inorganic formulations. The reviewed studies demonstrate that careful selection of photochemical mechanisms (*e.g.*, free-radical (meth)acrylic, thiol–ene, cycloaddition, or cationic) allows precise tuning of crosslinking density, degradation behavior, mechanical response, and surface chemistry. Beyond illustrating the breadth of available chemistries, several general design principles emerge from the studies discussed in this review. First, the

choice of photochemical mechanism should be aligned with the required network homogeneity and stress tolerance: chain-growth (meth)acrylate systems offer high reactivity and broad synthetic versatility but may induce shrinkage and residual stress, whereas step-growth thiol–ene chemistries provide improved network uniformity and reduced oxygen sensitivity, making them attractive for soft or biomedical systems. Second, optical penetration and curing depth must be considered in relation to fiber thickness and mat density; cationic systems with dark-curing capability can mitigate light-attenuation limitations in thick assemblies, while reversible photochemistries are more suitable for thin or surface-accessible architectures. Third, the relative timescales of jet stretching, solvent evaporation, and polymerization should be balanced to control internal stress and molecular orientation, particularly in *in situ* reactive electrospinning. Finally, application-specific constraints, such as biocompatibility, mechanical compliance, chemical resistance, or reconfigurability, should guide the selection of wavelength, initiator type, and reaction pathway. Together, these considerations provide a framework for rationally selecting photochemical strategies tailored to the structural, optical, and functional requirements of a given nanofibrous system.

Importantly, the nanofibrous morphology actively influences reaction efficiency and final properties, as high surface area, rapid solvent evaporation, and confined geometries influence polymerization kinetics and network formation in ways that differ fundamentally from bulk systems.

From a processing standpoint, photo-assisted electrospinning offers unique opportunities for temporal, spatial, and hierarchical control. Irradiation during jet flight, upon deposition, or as a post-processing step enables stabilization of otherwise unprocessable liquids, fixation of phase-separated or core–shell architectures, and selective surface functionalization without compromising the fibrous structure. The compatibility of photochemistry with patterned irradiation, photomasks, and wavelength-selective activation further opens routes toward multiscale structuring, gradient materials, and multifunctional membranes. In this respect, photo-induced processes transform electrospinning from a purely shaping technique into a reactive manufacturing platform.

Despite these advances, several challenges remain and define important directions for future research. First, a deeper understanding of reaction–flow–solidification coupling during electrospinning is still needed. Most current studies rely on empirical optimization, while predictive models linking photopolymerization kinetics, jet dynamics, and fiber morphology remain scarce. Addressing this gap will be essential for rational process design and reproducibility, particularly when scaling up.

Second, scalability and sustainability represent critical bottlenecks for translation beyond the laboratory. While needleless electrospinning, free-surface electrospinning, and roll-to-roll UV curing have shown promise, systematic studies integrating high-throughput electrospinning with energy-efficient and solvent-free photoprocesses are still limited. Future efforts should prioritize visible-light photochemistry, bio-based photoreactive monomers, and water-based formulations to align photo-assisted electrospinning with green chemistry principles.

Third, there is significant untapped potential in dynamic and adaptive fibrous systems. Photo-induced reactions enable not only permanent stabilization but also reversible crosslinking, latent reactivity, and multi-step functionalization. Exploiting these features could lead to reconfigurable nanofibrous materials capable of on-demand property changes, self-healing, or programmable degradation, which are concepts that are particularly appealing for soft robotics, wearable devices, and responsive biomedical scaffolds. However, dynamic and self-healing fibrous systems based on reversible photochemistry face intrinsic optical-depth limitations. In highly scattering nanofibrous mats, photon flux decays rapidly with depth, restricting efficient bond reformation primarily to regions near the irradiated surface. Consequently, bulk reconfiguration or healing in thick or multilayered architectures may be significantly less effective than in thin films or surface-grafted systems. Strategies such as longer-wavelength photochemistry,[159] light-induced frontal polymerization,[160] or hybrid dual-curing approaches[161] may help mitigate these constraints. Nevertheless, light attenuation remains a fundamental design parameter when translating dynamic photochemical concepts to scalable nanofibrous materials.

Finally, closer integration between photochemistry, electrospinning, and application-driven design will be crucial. While many studies demonstrate proof-of-concept functionalities, future work should emphasize structure–property–function relationships under realistic operating conditions, including long-term mechanical loading, biological environments, or cyclic stimuli. Multidisciplinary approaches combining polymer chemistry, process engineering, modeling, and advanced characterization will be key to unlocking the full potential of this field.

In conclusion, coupling electrospinning with photo-induced processes represents more than an incremental modification of an established technique: it constitutes a paradigm shift toward reactive, programmable, and multifunctional nanofibrous materials. Viewed through a soft matter lens, photo-assisted electrospinning represents a non-equilibrium, confinement-driven route to hierarchical materials in which interfacial chemistry and nanoscale structure jointly dictate macroscopic function. Continued advances in photochemistry, light sources, and scalable electrospinning technologies are expected to further consolidate this approach as a cornerstone in the development of next-generation soft matter systems for biomedical, environmental, energy, and smart-material applications.

Author contributions

T. N. Vu: visualization, writing; A. Vitale: conceptualization, resources, supervision, visualization, writing.

Conflicts of interest

There are no conflicts to declare.

Data availability

No primary research results, software or code have been included and no new data were generated or analysed as part of this review.

Acknowledgements

Part of this work was supported by EU Horizon Europe programme MSCA-DN Grant Agreement no. 101073432; funding was provided by the European Union. For the graphical abstract, icons for the application part were provided by Graphiqa, Freepik, Wichai.wi, Iconjam, bsd from https://www.flaticon.com.

References

1 C. Wang, W. Wang, H. Qi, Y. Dai, S. Jiang, B. Ding, X. Wang, C. Li, J. Zeng, T. Wu, H. Li, Y. Wang, Y. Zhao, W. Wang, Z. Li, X. Mo, H. Hou, L. Dong, H. Ma, Y. Liu, C. Su, J. Bai, W. Wu, G. Guo, G. Nie, N. Wang, H. Zhu, J. Bai, J. Fang, D. Liang, Z. Ba, G. Han, X. Lu, K. Wang, X. Zhang, W. Kang, N. Deng, W. Hu, W. Chen, X. Zhang, D. Yang, F. Wang, Y. Bian, Z. Liu, L. Zhang, X. Li, L. Li, Y. Li, H. Huang, X. Jia, X. Li, D. Yang, X. Jin, S. Li, X. Zhang, N. Tang, R. Hao, F. Tian, L. Mai, Y. Wei and J. Xue, *Prog. Mater. Sci.*, 2025, **154**, 101494.

2 D. Ji, Y. Lin, X. Guo, B. Ramasubramanian, R. Wang, N. Radacsi, R. Jose, X. Qin and S. Ramakrishna, *Nat. Rev. Methods Primers*, 2024, **4**, 1.

3 A. Nadaf, A. Gupta, N. Hasan, Fauziya, S. Ahmad, P. Kesharwani and F. J. Ahmad, *RSC Adv.*, 2022, **12**, 23808–23828.

4 H. M. Younes, H. Kadavil, H. M. Ismail, S. A. Adib, S. Zamani, R. G. Alany and A. A. Al-Kinani, *Pharmaceutics*, 2024, **16**, 32.

5 S. Chatani, C. J. Kloxin and C. N. Bowman, *Polym. Chem.*, 2014, **5**, 2187–2201.

6 M. A. S. N. Weerasinghe, T. Nwoko and D. Konkolewicz, *Chem. Sci.*, 2025, **16**, 5326–5352.

7 M. Babazadeh-Mamaqani, D. Razzaghi, H. Roghani-Mamaqani, A. Babaie, M. Rezaei, R. Hoogenboom and M. Salami-Kalajahi, *Prog. Mater. Sci.*, 2024, **146**, 101312.

8 J. Xue, T. Wu, Y. Dai and Y. Xia, *Chem. Rev.*, 2019, **119**, 5298–5415.

9 A. Keirouz, Z. Wang, V. S. Reddy, Z. K. Nagy, P. Vass, M. Buzgo, S. Ramakrishna and N. Radacsi, *Adv. Mater. Technol.*, 2023, **8**, 2201723.

10 H. M. Ibrahim and A. Klingner, *Polym. Test.*, 2020, **90**, 106647.

11 J. Lee, S. Moon, J. Lahann and K. J. Lee, *Macromol. Mater. Eng.*, 2023, **308**, 2300057.

12 Z. Yu, T. Fan, Y. Liu, L. Li, J. Liu, B. Yang, S. Ramakrishna and Y.-Z. Long, *Sep. Purif. Technol.*, 2024, **349**, 127773.

13 M. Rahmati, D. K. Mills, A. M. Urbanska, M. R. Saeb, J. R. Venugopal, S. Ramakrishna and M. Mozafari, *Prog. Mater. Sci.*, 2021, **117**, 100721.

14 F. Cheng, D. Song, H. Li, S. K. Ravi and S. C. Tan, *Adv. Funct. Mater.*, 2025, **35**, 2406950.

15 R. Bongiovanni, S. Dalle Vacche and A. Vitale, *Polymers*, 2021, **13**(14), 2293.

16 J. W. Verhoeven, *Pure Appl. Chem.*, 1996, **68**, 2223–2286.

17 Y. Yagci, S. Jockusch and N. J. Turro, *Macromolecules*, 2010, **43**, 6245–6260.

18 M. Höfer, N. Moszner and R. Liska, *J. Polym. Sci., Part A: Polym. Chem.*, 2008, **46**, 6916–6927.

19 A. B. Lowe, *Polym. Chem.*, 2010, **1**, 17–36.

20 N. Corrigan, J. Yeow, P. Judzewitsch, J. Xu and C. Boyer, *Angew. Chem., Int. Ed.*, 2019, **58**, 5170–5189.

21 C. Aydogan, G. Yilmaz, A. Shegiwal, D. M. Haddleton and Y. Yagci, *Angew. Chem., Int. Ed.*, 2022, **61**, e202117377.

22 X. Li, J. Zhou, Z. Quan, L. Wang, F. Li, X. Qin and J. Yu, *Dyes Pigm.*, 2021, **193**, 109462.

23 T. Blachowicz and A. Ehrmann, *Membranes*, 2023, **13**(4), 441.

24 M. Richard-Lacroix and C. Pellerin, *Macromolecules*, 2013, **46**, 9473–9493.

25 X. Wen, J. Xiong, Z. Sun, L. Wang, J. Yu and X. Qin, *Engineering*, 2023, **29**, 179.

26 S. Tripatanasuwan, Z. Zhong and D. H. Reneker, *Polymer*, 2007, **48**, 5742–5746.

27 F. Fang, H. Wang, H. Wang, W. M. Huang, Y. Chen, N. Cai, X. Chen and X. Chen, *Micromachines*, 2021, **12**(8), 920.

28 T. Kawamoto, D.-T. Van-Pham, H. Nakanishi, T. Norisuye, Q. Tran-Cong-Miyata and K. Fukao, *Polym. J.*, 2014, **46**, 819–822.

29 H. Lu, J. W. Stansbury and C. N. Bowman, *J. Dent. Res.*, 2005, **84**, 822–826.

30 C. N. Bowman and C. J. Kloxin, *AIChE J.*, 2008, **54**, 2775–2795.

31 T. Kongkhlang, K. Tashiro, M. Kotaki and S. Chirachanchai, *J. Am. Chem. Soc.*, 2008, **130**, 15460–15466.

32 D. H. Reneker, A. L. Yarin, E. Zussman and H. Xu, *Adv. Appl. Mech.*, 2007, **41**, 43–195.

33 A. W. Laramée, J. Chen, M. Le Faou and C. Pellerin, *Polymer*, 2025, **318**, 127976.

34 R. Wu, J.-F. Zhang, Y. Fan, D. Stoute, T. Lallier and X. Xu, *Biomed. Mater.*, 2011, **6**, 035004.

35 M. Montinaro, V. Fasano, M. Moffa, A. Camposeo, L. Persano, M. Lauricella, S. Succi and D. Pisignano, *Soft Matter*, 2015, **11**, 3424–3431.

36 S. Lei, L. Wang, R. Wang, X. Qin and J. Yu, *Sci. China Technol. Sci.*, 2022, **65**, 481–489.

37 X. Zhu, Q. Niu, Y. Xu, G. Wu, G. Li, J. Nie and G. Ma, *J. Photochem. Photobiol., A*, 2018, **353**, 101–107.

38 K. Shanmuganathan, R. K. Sankhagowit, P. Iyer and C. J. Ellison, *Chem. Mater.*, 2011, **23**, 4726–4732.

39 K. Shanmuganathan, S. M. Elliot, A. P. Lane and C. J. Ellison, *ACS Appl. Mater. Interfaces*, 2014, **6**, 14259–14265.

40 P. Kianfar, H. Q. Nguyen Trieu, S. Dalle Vacche, L. Tsantilis, R. Bongiovanni and A. Vitale, *Eur. Polym. J.*, 2022, **177**, 111453.

41 D. W. Janes, K. Shanmuganathan, D. Y. Chou and C. J. Ellison, *ACS Macro Lett.*, 2012, **1**, 1138–1142.
42 S.-S. Kim, C. M. Lau, L. M. Lillie, W. B. Tolman, T. M. Reineke and C. J. Ellison, *ACS Appl. Polym. Mater.*, 2019, **1**, 2933–2942.
43 H. Wang, Y. Feng, W. Yuan, H. Zhao, Z. Fang, M. Khan and J. Guo, *Sci. China Phys. Mech. Astron.*, 2012, **55**, 1189–1193.
44 H. Wang, Y. Feng, B. An, W. Zhang, M. Sun, Z. Fang, W. Yuan and M. Khan, *J. Mater. Sci.: Mater. Med.*, 2012, **23**, 1499–1510.
45 H. R. Ashjari, A. Ahmadi and M. S. S. Dorraji, *Korean J. Chem. Eng.*, 2018, **35**, 289–297.
46 D. O. Miranda, M. F. Dorneles and R. L. Oréfice, *Polym. Int.*, 2023, **72**, 434–439.
47 Q. Niu, L. Zeng, X. Mu, J. Nie and G. Ma, *J. Ind. Eng. Chem.*, 2016, **34**, 337–343.
48 Q. Niu, X. Zhu, Y. Tang, J. Nie and G. Ma, *Mater. Sci. Eng., C*, 2017, **77**, 326–332.
49 J. Zhou, Y. Liu, T. Jiao, R. Xing, Z. Yang, J. Fan, J. Liu, B. Li and Q. Peng, *Colloids Surf., A*, 2018, **538**, 7–13.
50 H. M. Ismail, S. Zamani, M. A. Elrayess, W. Kafienah and H. M. Younes, *Polymers*, 2018, **10**, 455.
51 S. H. Kim, S.-H. Kim, S. Nair and E. Moore, *Macromolecules*, 2005, **38**, 3719–3723.
52 D. O. Miranda, M. F. Dorneles and R. L. Oréfice, *Polymer*, 2020, **200**, 122590.
53 L. Qi, C.-Y. Guo, M.-G. H. Fu, Y. Zhang, L. Yin, L. Wu, J. Liu and X. Zhang, *Polymers*, 2019, **11**, 2055.
54 L. Qi, J. Liu, Y. Yang, C. Guo, M. Huangfu and Y. Zhang, *J. Appl. Polym. Sci.*, 2021, **138**, 50048.
55 L. Qi, C. Guo, Y. Zhang, L. Yin, L. Wu, J. Liu and X. Zhang, *J. Mater. Sci.: Mater. Electron.*, 2020, **31**, 17647–17658.
56 X. Xu, J.-F. Zhang and Y. Fan, *Biomacromolecules*, 2010, **11**, 2283–2289.
57 M. K. Cho, B. S. Singu, Y. H. Na and K. R. Yoon, *J. Appl. Polym. Sci.*, 2016, **133**, 42914.
58 Z. Ahmadipour, M. S. Seyed Dorraji, H. R. Ashjari, F. Dodangeh and M. H. Rasoulifard, *Sci. Rep.*, 2023, **13**, 9741.
59 X. Liao, Z. Xiang, Y. Lei, Z. Zhu, J. Guo, S. Lin and J. Shang, *Polymer*, 2022, **252**, 124925.
60 P. Rao N, J. K. Ajish and K. S. A. Kumar, *Int. J. Biol. Macromol.*, 2025, **329**, 147793.
61 X. Chen, B. Lu, D. Zhou, M. Shao, W. Xu and Y. Zhou, *Int. J. Biol. Macromol.*, 2020, **155**, 903–910.
62 Y. Zhou, Q. Dong, H. Yang, X. Liu, X. Yin, Y. Tao, Z. Bai and W. Xu, *Carbohydr. Polym.*, 2017, **168**, 220–226.
63 J.-F. Zhang, Y. Wang, M. L. Lam, R. J. McKinnnie, W. C. Claycomb and X. Xu, *Mater. Today Commun.*, 2017, **13**, 306–316.
64 Q. Wang, L. Yuan, K. Zhu, L. Ren and X. Yuan, *Chem. Res. Chin. Univ.*, 2025, **41**, 620–628.
65 E. Shamirzaei Jeshvaghani, L. Ghasemi-Mobarakeh, R. Mansurnezhad, F. Ajalloueian, M. Kharaziha, M. Dinari, M. Sami Jokandan and I. S. Chronakis, *J. Biomed. Mater. Res., Part B*, 2018, **106**, 2371–2383.
66 D. Y. Deniz, M. V. Kahraman, S. Erdem Kuruca, M. Suleymanoglu and A. Gungor, *Int. J. Polym. Mater. Polym. Biomater.*, 2015, **64**, 727–732.
67 T. Ahmadi, A. Monshi, V. Mortazavi, M. H. Fathi, S. Sharifi, M. Kharaziha, L. Khazdooz, A. Zarei and M. Taghian Dehaghani, *Mater. Sci. Eng., C*, 2020, **106**, 110172.
68 J. Pukkao, P. Pisitsak, W. Inprasit and T. Inprasit, *Fibers Polym.*, 2022, **23**, 58–67.
69 N. Kassenova, S. Kalybekkyzy, M. V. Kahraman, A. Mentbayeva and Z. Bakenov, *J. Power Sources*, 2022, **520**, 230896.
70 Y. Yerkinbekova, S. Kalybekkyzy, N. Tolganbek, M. V. Kahraman, Z. Bakenov and A. Mentbayeva, *Sci. Rep.*, 2022, **12**, 18272.
71 X. He, L. Zang, Y. Xin and Y. Zou, *Appl. Res.*, 2023, **2**, e202300030.
72 P. Kianfar, A. Vitale, S. Dalle Vacche and R. Bongiovanni, *J. Mater. Sci.*, 2021, **56**, 1879–1896.
73 G. Fredi, P. Kianfar, S. Dalle Vacche, A. Pegoretti and A. Vitale, *Polymers*, 2021, **13**, 2979.
74 P. Kianfar, S. Dalle Vacche, G. Fredi, R. Bongiovanni and A. Vitale, *Monatsh. Chem.*, 2025, 1–11.
75 P. Kianfar, S. Dalle Vacche, R. Bongiovanni, C. Mollea, F. Bosco, Z. Najmi, A. C. Scalia, A. Cochis and A. Vitale, *ACS Appl. Polym. Mater.*, 2024, **6**, 14749–14759.
76 E. Maccaferri, A. Canciani, L. Mazzocchetti, T. Benelli, L. Giorgini and S. Albonetti, *Membranes*, 2023, **13**, 212.
77 S. Chen, Y. Liu, Q. Dong, Y. Zhou, X. Yin, D. Chen, C. Xu and W. Xu, *J. Photopolym. Sci. Technol.*, 2016, **29**, 841–847.
78 J. S. Stephens-Altus, P. Sundelacruz, M. L. Rowland and J. L. West, *J. Biomed. Mater. Res., Part A*, 2011, **98A**, 167–176.
79 Y. Dou, S. Wang, M. E. Gibril and F. Kong, *Chem. Eng. J.*, 2024, **481**, 148435.
80 Y. Jin, D. Yang, Y. Zhou, G. Ma and J. Nie, *J. Appl. Polym. Sci.*, 2008, **109**, 3337–3343.
81 M. Zhu, R. Xiong and C. Huang, *Carbohydr. Polym.*, 2019, **205**, 55–62.
82 Y. Zhou, K. Liang, C. Zhang, J. Li, H. Yang, X. Liu, X. Yin, D. Chen, W. Xu and P. Xiao, *Cellulose*, 2017, **24**, 4253–4262.
83 D. Poustka, M. Liegertová, R. Herma, M. Munzarová and J. Malý, *Polym. Bull.*, 2026, **83**, 117.
84 K. C. de Castro, J. Burga-Sánchez, M. G. N. Campos and L. H. I. Mei, *RSC Adv.*, 2020, **10**, 31271–31279.
85 H. G. Sundararaghavan, R. B. Metter and J. A. Burdick, *Macromol. Biosci.*, 2010, **10**, 265–270.
86 X. Yang, D. Yang, X. Zhu, J. Nie and G. Ma, *Eur. Polym. J.*, 2019, **113**, 142–147.
87 S. I. Jeong, O. Jeon, M. D. Krebs, M. C. Hill, E. Alsberg, S. I. Jeong, O. Jeon, M. D. Krebs, M. C. Hill and E. Alsberg, *Eur. Cell Mater.*, 2012, **24**, 331–343.
88 A. Nawaz, Z. Ahmad, M. B. Taj, A. Ihsan and M. Tasleem, *Mater. Res. Bull.*, 2026, **197**, 113930.
89 A. A. Ayoub, A. H. Mahmoud, J. S. Ribeiro, A. Daghrery, J. Xu, J. C. Fenno, A. Schwendeman, H. Sasaki, R. Dal-Fabbro and M. C. Bottino, *Int. J. Mol. Sci.*, 2022, **23**, 13761.

90 B. Li, Y. Chen, J. He, J. Zhang, S. Wang, W. Xiao, Z. Liu and X. Liao, *ACS Biomater. Sci. Eng.*, 2020, **6**, 6737–6747.
91 J. Liang, H. Chen, Z. Guo, P. Dijkstra, D. Grijpma and A. Poot, *Eur. Polym. J.*, 2021, **152**, 110471.
92 E. Pilavci, M. Ayran, D. Ulubay, E. Kaya, G. Tinaz, O. Bingol Ozakpinar, A. Sancakli and O. Gunduz, *J. Bioact. Compat. Polym.*, 2023, **38**, 3–24.
93 A. H. Mahmoud, Y. Han, R. Dal-Fabbro, A. Daghrery, J. Xu, D. Kaigler, S. B. Bhaduri, J. Malda and M. C. Bottino, *ACS Appl. Mater. Interfaces*, 2023, **15**, 32121–32135.
94 S. S. Namazi, P. H. C. de Oliveira, N. J. McDonald, B. Cavalcanti, H. Sasaki, M. C. Bottino and R. Dal-Fabbro, *Odontology*, 2025, 1–10.
95 C. Li, W. Li, R. Deng, L. Huang, Y. Song, X. Wei, B. Xu, G. Cui, Z. Chen and J. Yu, *Adv. Fiber Mater.*, 2025, 1–26.
96 R. M. Sturm, Y. Huo, F. Yiu, Y. Gu, R. Afshari, Z. Zhong, R. Jimenez, R. Jung, A. Cabuan, K. Shukla, K. Harrison, J. Su, G. E. Aninwene II, V. Lee, M. Ghovvati, K. Shariati, N. Jackson, S. Li and N. Annabi, *Adv. Healthcare Mater.*, 2025, **14**, 2500651.
97 P. Coimbra, P. Santos, P. Alves, S. P. Miguel, M. P. Carvalho, K. D. de Sá, I. J. Correia and P. Ferreira, *Colloids Surf., B*, 2017, **159**, 7–15.
98 Z. Xie, W.-C. Li, X.-M. Sun, Z.-Y. Lin and L. Ren, *ACS Appl. Polym. Mater.*, 2022, **4**, 987–998.
99 P. Alves, M. Santos, S. Mendes, S. P. Miguel, K. D. de Sá, C. S. D. Cabral, I. J. Correia and P. Ferreira, *Polymers*, 2019, **11**, 653.
100 X. He, R. Wang, X. Liu, R. Peng, B. Zhou, L. Wang, X. Wei, S. Wang, J. Bai, Q. Feng, F. Zhou, H. Liu and Y. Fan, *ACS Nano*, 2025, **19**, 20841–20862.
101 M. R. Badrak, J. Senanayake, A. Zunnu Rain and H. G. Sundararaghavan, *J. Biomater. Appl.*, 2025, **40**, 307–323.
102 S. Qiu, S. Zhang, Y. He, T. Li, Y. Feng and J. Xu, *J. Appl. Polym. Sci.*, 2026, **143**, e58137.
103 M. D. Popov Pereira da Cunha, A. A. Aldana and G. A. Abraham, *Mater. Lett.: X*, 2021, **12**, 100115.
104 L. Ye, X. Wu, X. Geng, Y. Duan, Y. Gu, A. Zhang, J. Zhang and Z. Feng, *Chin. J. Polym. Sci.*, 2010, **28**, 829–840.
105 L. Jun, Y. Zhang, Y. Hao, L. Cheng and J. J. Zhang., *J. Appl. Polym. Sci.*, 2009, **112**, 2247–2254.
106 M. B. Bazbouz, H. Liang and G. Tronci, *Mater. Sci. Eng., C*, 2018, **91**, 541–555.
107 A. Houben, P. Roose, H. Van den Bergen, H. Declercq, J. Van Hoorick, P. Gruber, A. Ovsianikov, D. Bontinck, S. Van Vlierberghe and P. Dubruel, *Mater. Today Chem.*, 2017, **4**, 84–89.
108 A. R. Tan, J. L. Ifkovits, B. M. Baker, D. M. Brey, R. L. Mauck and J. A. Burdick, *J. Biomed. Mater. Res., Part A*, 2008, **87A**, 1034–1043.
109 J. L. Ifkovits, R. F. Padera and J. A. Burdick, *Biomed. Mater.*, 2008, **3**, 034104.
110 R. B. Metter, J. L. Ifkovits, K. Hou, L. Vincent, B. Hsu, L. Wang, R. L. Mauck and J. A. Burdick, *Acta Biomater.*, 2010, **6**, 1219–1226.
111 J. Yao, O. T. Picot, N. F. Hughes-Brittain, C. W. M. Bastiaansen and T. Peijs, *Eur. Polym. J.*, 2016, **84**, 642–651.
112 D. Wu, X. Li, Y. Zhang, X. Cheng, Z. Long, L. Ren, X. Xia, Q. Wang, J. Li, P. Lv, Q. Feng and Q. Wei, *Adv. Sci.*, 2024, **11**, 2400557.
113 C. E. Hoyle and C. N. Bowman, *Angew. Chem., Int. Ed.*, 2010, **49**, 1540–1573.
114 S. Sharma, N. Monteleone, I. Kopyeva and S. J. Bryant, *J. Appl. Polym. Sci.*, 2021, **138**, 50786.
115 Y.-T. Tsai, C.-W. Chang and Y.-C. Yeh, *Biomater. Sci.*, 2020, **8**, 4728–4738.
116 A. Battistella, M. Linger, R. D. Johnson, M. Overton, A. Sallee, R. Jain, B. Antreasian, Y. Ding and W. Tan, *Biomed. Mater.*, 2025, **20**, 065019.
117 L. De Grave, K. V. Bernaerts and S. Van Vlierberghe, *Next Mater.*, 2024, **3**, 100172.
118 K. Gwon, W. I. Choi, S. Lee, J. S. Lee and J. H. Shin, *Biomater. Sci.*, 2021, **9**, 8160–8170.
119 A. Vitale, G. Massaglia, A. Chiodoni, R. Bongiovanni, C. F. Pirri and M. Quaglio, *ACS Appl. Mater. Interfaces*, 2019, **11**, 24544–24551.
120 P. Kianfar, A. Bakry, S. Dalle Vacche, R. Bongiovanni and A. Vitale, *J. Mater. Sci.*, 2024, **59**, 3711–3724.
121 S. Briggs, S. Herting, G. Fletcher, R. Gruenbaum and D. J. Maitland, *Nanomaterials*, 2022, **12**, 406.
122 X. Ding, Y. G. Chen, E. Goltz, N. Gantumur and B. P. Lee, *Macromol. Biosci.*, 2025, **25**, e00308.
123 H.-A. Christ and H. Menzel, *Macromol. Mater. Eng.*, 2023, **308**, 2200430.
124 C. Yi, R. Nirmala, R. Navamathavan, X.-D. Li and H.-Y. Kim, *J. Nanosci. Nanotechnol.*, 2011, **11**, 8474–8480.
125 O. Frateur, J. Becelaere, R. Merckx, J. F. R. Van Guyse, M. Purino, R. Hoogenboom and K. De Clerck, *Eur. Polym. J.*, 2024, **212**, 113076.
126 Y. Liu, B. Bolger, P. A. Cahill and G. B. McGuinness, *Mater. Lett.*, 2009, **63**, 419–421.
127 S. Takahara, N. Iwamura, Y. Ema, Y. Sato, M. Mizukoshi, T. Nagano and N. Ichikuni, *Polym. Adv. Technol.*, 2015, **26**, 338–344.
128 S. Fujisawa, M. Yamamoto, D. Kashiwai, P. Azari, Y. Y. Khaw, S. N. Gan and S. Takahara, *J. Photopolym. Sci. Technol.*, 2018, **31**, 569–574.
129 J. Zeng, H. Hou, J. H. Wendorff and A. Greiner, *Macromol. Rapid Commun.*, 2005, **26**, 1557–1562.
130 Y. Chen, Z. Sun, Z. Xu, H. Lin, J. Gao, J. Song, Z. Li, R. Huang, Y. Geng, D. Wu and Q. Feng, *J. Membr. Sci.*, 2025, **727**, 124024.
131 J. Ham, K. M. Lee, J. Ko, K. Lee and W.-G. Koh, *ACS Appl. Polym. Mater.*, 2023, **5**, 625–634.
132 Y. Li, M. Vergaelen, E. Schoolaert, R. Hoogenboom and K. De Clerck, *Eur. Polym. J.*, 2019, **112**, 24–30.
133 P. Kianfar, A. Vitale, S. Dalle Vacche and R. Bongiovanni, *Carbohydr. Polym.*, 2019, **217**, 144–151.
134 S. Krause, R. Dersch, J. H. Wendorff and H. Finkelmann, *Macromol. Rapid Commun.*, 2007, **28**, 2062–2068.
135 J. P. Yapor, A. Alharby, C. Gentry-Weeks, M. M. Reynolds, A. K. M. M. Alam and Y. V. Li, *ACS Omega*, 2017, **2**, 7334–7342.

136 M. O. Kim and J. S. Lee, *Fash Text*, 2019, **6**, 27.
137 M. Sangermano, I. Roppolo and A. Chiappone, *Polymers*, 2018, **10**, 136.
138 A. Iregui, L. Irusta, O. Llorente, L. Martin, T. Calvo-Correas, A. Eceiza and A. González, *Eur. Polym. J.*, 2017, **94**, 376–383.
139 I. Razquin, A. Iregui, M. Cobos, J. Latasa, A. Eceiza, K. González, L. Martin, A. J. Müller, A. González and L. Irusta, *Polymer*, 2023, **282**, 126160.
140 W.-Y. Zhang, X.-Z. Xiao, C. Lv, J. Zhao, G. Wang, X. Gu, R. Zhang, B.-B. Xu, D.-D. Zhang, A.-W. Li, Y.-L. Zhang and H.-B. Sun, *Macromol. Res.*, 2013, **21**, 306–310.
141 M. F. Attia, A. S. Montaser, M. Arifuzzaman, M. Pitz, K. Jlassi, A. Alexander-Bryant, S. S. Kelly, F. Alexis and D. C. Whitehead, *Polymers*, 2021, **13**, 1863.
142 K. Arroub, I. Gessner, T. Fischer and S. Mathur, *Adv. Eng. Mater.*, 2021, **23**, 2100221.
143 T. R. Correia, P. Ferreira, R. Vaz, P. Alves, M. M. Figueiredo, I. J. Correia and P. Coimbra, *Int. J. Biol. Macromol.*, 2016, **93**, 1539–1548.
144 Y. Xu, H. Lu, C. Sun, L. Zou, H. Yin and W. Li, *Macromol. Mater. Eng.*, 2020, **305**, 2000344.
145 J. Lee, B. Ryu, E. Yeom and W.-G. Koh, *Sens. Actuators, B*, 2025, **443**, 138211.
146 Q. Niu, X. Mu, J. Nie and G. Ma, *J. Ind. Eng. Chem.*, 2016, **38**, 193–199.
147 X. Zhu, H. Zhang, J. Nie and G. Ma, *J. Ind. Eng. Chem.*, 2017, **45**, 334–337.
148 Y. Song and S. Lee, *Fibers Polym.*, 2023, **24**, 4061–4071.
149 Y. Song and S. Lee, *Fibers Polym.*, 2026, **27**, 519–531.
150 P. V. Mayuri, A. Bhatt, R. Joseph and P. Ramesh, *Mater. Sci. Eng., C*, 2016, **60**, 19–29.
151 P. V. Mayuri, A. Bhatt and P. Ramesh, *J. Appl. Polym. Sci.*, 2019, **136**, 47057.
152 P. V. Mayuri, A. Bhatt, A. Sabareeswaran and R. Parameswaran, *Mater. Today Commun.*, 2021, **26**, 102075.
153 K. Dziemidowicz, S. Brocchini and G. R. Williams, *Int. J. Pharm.*, 2021, **597**, 120231.
154 D.-L. Versace, J. Ramier, D. Grande, S. A. Andaloussi, P. Dubot, N. Hobeika, J.-P. Malval, J. Lalevee, E. Renard and V. Langlois, *Adv. Healthcare Mater.*, 2013, **2**, 1008–1018.
155 L. Ribba, L. Tamayo, M. Flores, A. Riveros, M. J. Kogan, E. Cerda and S. Goyanes, *J. Appl. Polym. Sci.*, 2019, **136**, 47369.
156 J. A. Talamo Ruiz, P. Kianfar, S. Dalle Vacche, R. Bongiovanni and A. Vitale, *J. Membr. Sci.*, 2025, **734**, 124457.
157 X. Wang, Y. Liu, M. Zhang, Z. Luo and D. Yang, *Ind. Eng. Chem. Res.*, 2020, **59**, 10894–10903.
158 W. Yuan, M. Ding, J. Weng, T. Xue, M. Xie, P. Zhang, J. Mu and P. Zhou, *Chem. Eng. J.*, 2025, **514**, 163142.
159 G. Ma, J. Luo and J. Qu, *Prog. Org. Coat.*, 2024, **189**, 108296.
160 H. M. Dizman, A. Vitale and R. Bongiovanni, *Polym. Compos.*, 2026, 1–11.
161 W. Gao, Y. Guo, J. Cui, C. Liang, Z. Lu, S. Feng, Y. Sun, Q. Xia and B. Zhang, *Addit. Manuf.*, 2024, **85**, 104142.